THESIS


HYDROLOGIC MODELING OF A SMALL UNGAUGED BASIN IN THE SAHEL: UNIQUE

CALIBRATION AND RESULTS

Submitted by

Mikell Warms

Department of Civil and Environmental Engineering

In partial fulfillment of the requirements

For the Degree of Master of Science

Colorado State University

Fort Collins, Colorado

Spring 2014

Master's Committee:

    Advisor: Jorge. A. Ramirez

    Neil S. Grigg
    Stephanie Kampf

ABSTRACT

HYDROLOGIC MODELING OF A SMALL UNGAUGED BASIN IN THE SAHEL: UNIQUE

CALIBRATION AND RESULTS

The Sahelian region of Africa is a geographic belt directly south of the Sahara, connecting the desert to the wetter Sudanian and Guinean savannas to the South. The region is semi-arid, receiving only 300-600 mm of precipitation on average annually. In addition, the Sahel experiences severe dry seasons (7-9 months) with little to no rain. Measurement stations in the region are scarce and reliable data is often difficult to obtain. It is common for drainage basins throughout many parts of the world to be ungauged or gauged but deteriorating. Conventional hydrologic modeling techniques to calibrate and verify basin parameters are rarely applicable in these cases. This problem is exacerbated when human-induced changes to the land surface and climate change impacts lead to increased uncertainty.

A recent hydrologic regime shift in parts of the Sahel has been observed and is the basis for this study. Traditionally, a lack of perennial water sources in the region limited settlement, and only seasonal grazing was commonplace. However, many of the previously ephemeral lakes in the region have become perennial or less drastically ephemeral, and settlements have begun to appear in these locations. Hypotheses of how this regime shift occurred, or whether this trend will continue were tested with a calibrated hydrologic model. This study will: (1) address briefly the difficulty in calibrating hydrologic models in ungauged basins; (2) share the results of a unique calibration procedure; and (3) test project hypotheses using the calibrated hydrologic model in a case study of a small lake basin in Northern Mali.

# ACKNOWLEDGEMENTS

TABLE OF CONTENTS

# LIST OF TABLES

# LIST OF FIGURES

## 1. Background

*1.1: The Sahel*

The Sahelian region of Africa is the geographic belt directly south of the Sahara extending from the Atlantic Ocean to the Red Sea, connecting the desert to the wetter Sudanian savannas of the South [*Figure 1.1*].
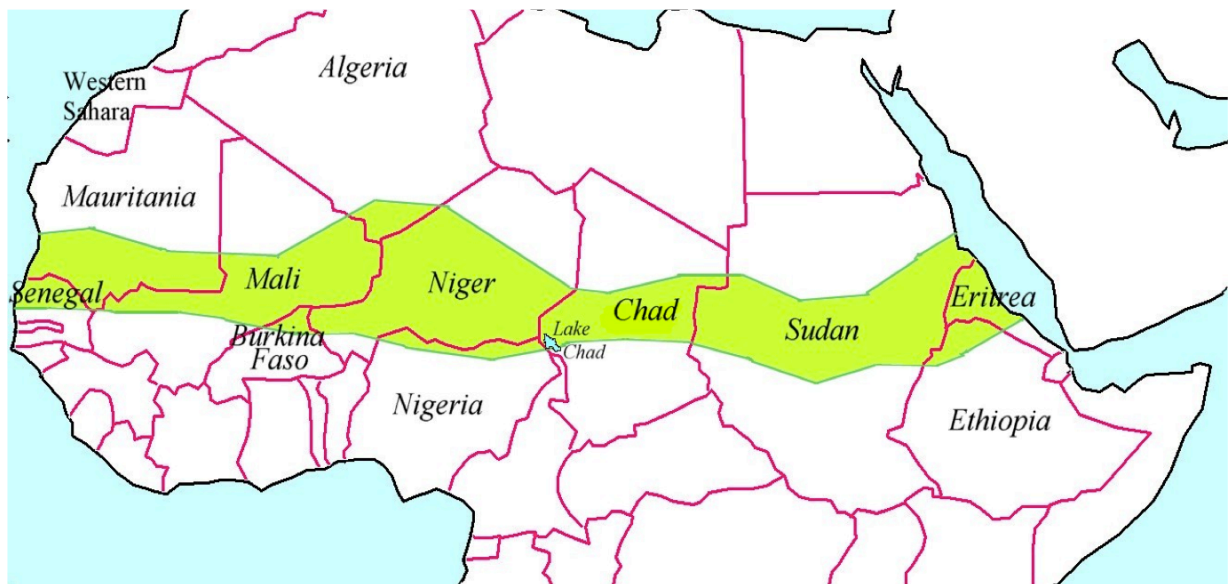


*Figure 1.1: The Sahelian region of Africa*

Although no exact boundary is defined, the typical consensus is that the Sahel lies between the 300 and 600 mm mean annual precipitation (MAP) isohyets. In addition, the Sahel experiences severe dry seasons of 6 to 9 months with little to no rain, receiving almost all of its precipitation during the short wet season from June to September [*Figure 1.2*] (*Frappart et al. 2009, Lebel et al. 1997*).
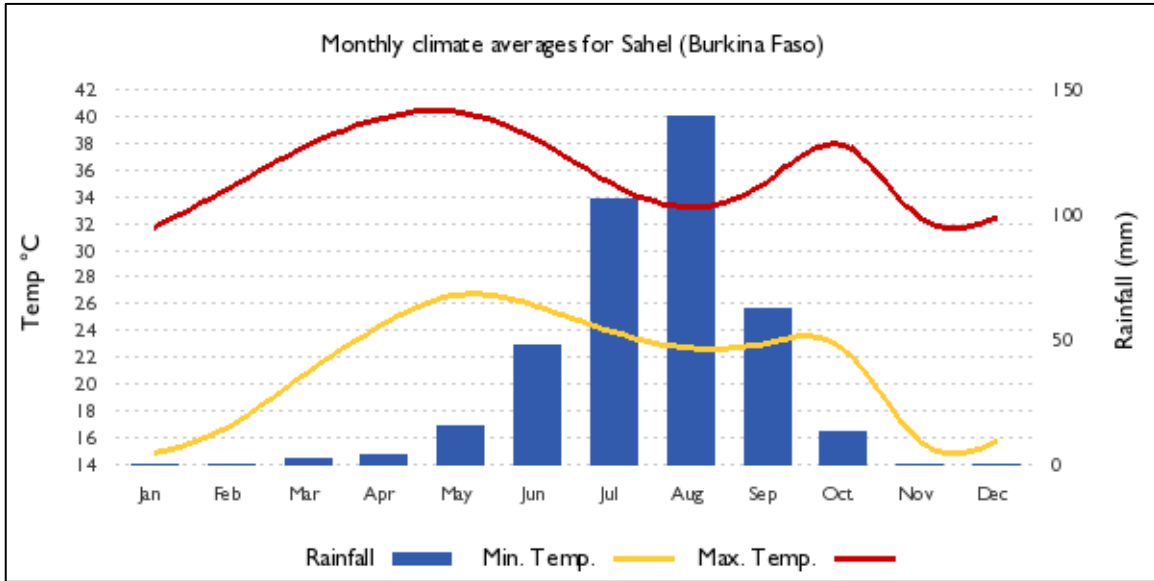
*Figure 1.2*: Long-term average climate data for the Sahel in Burkina Faso (adapted from WorldClim 50-year monthly climate data)

West African Monsoonal convective systems are the predominant rainfall mechanism in the Sahel, delivering high intensity bursts of precipitation over short durations (*Mathon et al. 2002, Lebel et al. 1997).* Due to the high impact of intense rains from convective storm systems, crust formation is prevalent in many areas of the Sahel. Soil crusts decrease the infiltration rate as well as the infiltration capacity of topsoil; therefore high volumes of surface runoff are commonplace [*Figure 1.3*] (*Hoogmoed et al. 1984, Valentin et al. 2004*).
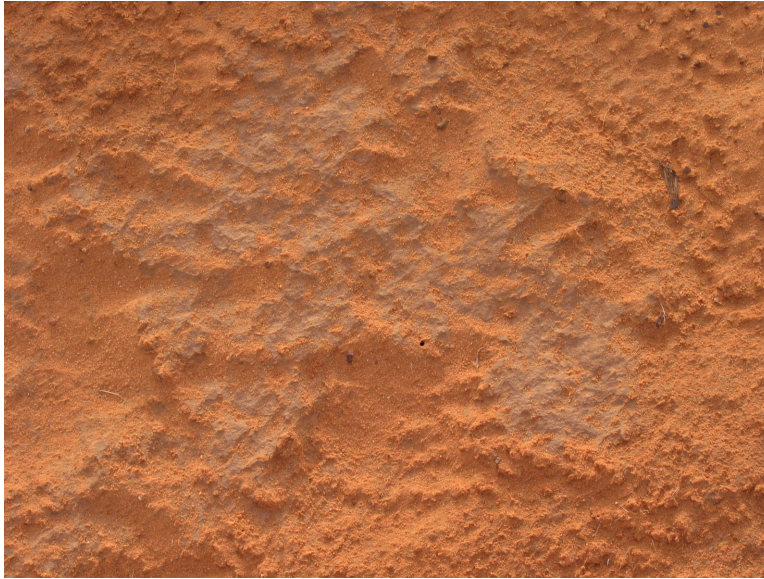
*Figure 1.3: Soil crust formation in the Sahel near Niamey, Niger*

Vegetation in the Sahel consists mainly of grass annuals. Combined tree and shrub density tends to be less than 5 percent of canopy cover (*Hermann et al. 2005a, Hiernaux et al. 2008*). Because limited rainfall limits the productivity of Sahelian vegetation, soil nutrients in the region are readily available. As such, Sahelian vegetation has been and still is a prized grazing resource in the region due to its high nutrient value and digestibility (*Le Houérou, 1980, 1989)*. Historically, drinking water for domestic animals has been abundant during and immediately after the rainy season due to the presence of ephemeral surface pools. However, once the ephemeral pools begin to evaporate following the departure of the rains, herds need to return to the wetter Sudanian and Guinean regions in the South. Cattle gain most of their body mass during the short rainy season in the Sahel, and upon returning hundreds of kilometers South, herds transport Sahelian nutrients that indirectly sustain grain production with nutrient-rich manure (*Dembele et al. 2006, Turner et al.*

*2000*). In this regard, the Sahel provides an extremely valuable resource for the entire region.

*1.2: Droughts and Hydrologic Regime Shift*

During the past half-century, two severe droughts struck the Sahel: the first occurred in 1968-1973 and the other, often called the "Great Sahelian Drought", occurred in 1983-1985. These two droughts occurred within a dry period of approximately 25 years from 1968-1993, following a wet period of approximately 20 years from 1948-1968 [*Figure 1.4*] (*Nicholson 2001, Le Barbe et al. 2002*). They had an extremely detrimental effect on the populations of vegetation, crops, and domestic animals. Woody plant populations were especially devastated (*Olsson 1993, Hiernaux et al. 2008*). Beginning in the 1990s, precipitation has more or less returned to the century average (*Frappart et al. 2009, Nicholson 2005, Olsson et al. 2005*).

Rather than rainfall deficits leading to a decrease in runoff as would be expected, in many parts of the Sahel there have been reports of increased river discharges and increased flooding of ponds and lakes (*Descroix et al. 2009*). Following the Great Sahelian Drought (GSD), field observations in the central and Northern Sahel have shown that ephemeral pools began to persist further into the dry season even prior to the return of average rainfall, some of them even becoming perennial (*Mahe et al. 2003, Gardelle et al. 2009*). In the Southern Sahel, these increases as well as evidence of an increase in the water table of endorheic areas, such as in the Niamey region of Southwestern Niger, have also been reported (*Leduc et al., 2001*). This oft called "Sahelian Paradox" has been intensely studied (*Gardelle et al. 2009, Descroix et al. 2009, Leblanc et al. 2008, Favrueu et al. 2002,*

*2009, Leduc et al. 2001, Mahe et al. 2003, 2005*), and while both regions have experienced increased river flows, surface runoff and pond volumes, the respective mechanisms of these increases are different.
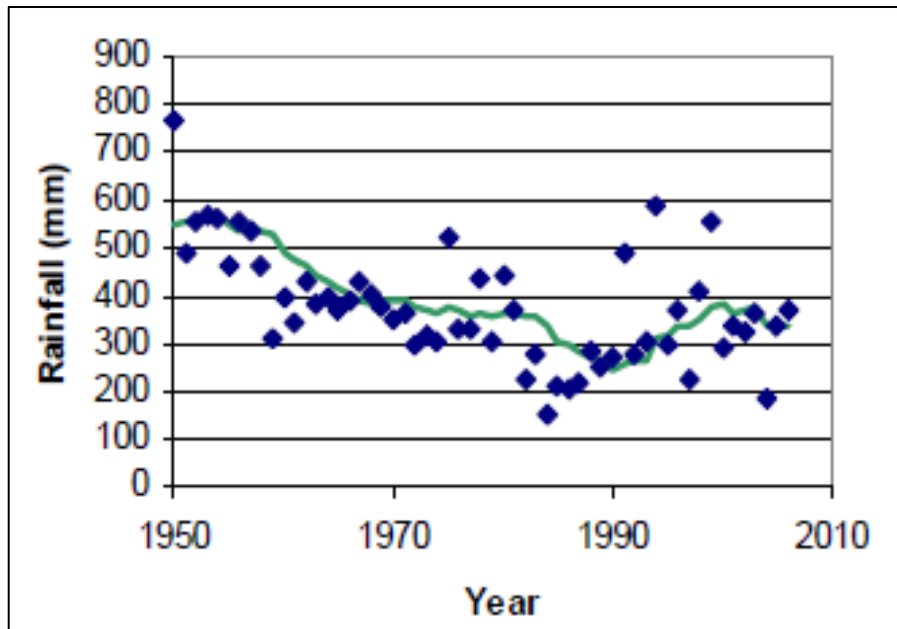


*Figure 1.4: Sahelian annual precipitation over time. Blue symbols indicate annual rainfall; Solid line indicates a 10-year prior average. (Adapted from Hanan et al. 2009--Project Proposal)*

In Niamey, drought-induced mortality and human clearing of native vegetation over the past few decades has increased surface runoff in the area. Because this region is endorheic, surface runoff concentrates in temporary ponds and then infiltrates to the rising water table (*Leduc et al 2001, Favreau et al 2002*). In some areas, low-lying depressions have become hydraulically connected to the water table, causing temporary recharge pools to exist longer into the dry season. Contrastingly in the Central and Northern Sahel, a rising water table is not the cause of this phenomenon. While the causes in this region are still

somewhat up for debate, most agree that the lasting impact of the severe droughts of the past half century on the woody plant vegetation population—which had historically grown on shallow soils and hardpan outcrops—and its effect on surface runoff are the main cause. The hardpan surface is an outcropping of the "continental terminal," which consists of sand, silt, clay, and lateritic intercalations which lay above the metamorphic and granitic base (*Leduc & Desconnets, 1994*). Surface runoff flows downstream and pools in depressions on top of the impervious continental terminal. The runoff volume has increased such that the previously ephemeral pools are large enough that they are sustained through the dry summer months (*Gardelle et al. 2009)*. It is also argued that cropland expansion and an increase in pastoral use have an effect on increasing surface runoff, but that effect is generally seen as secondary (*Hermann et al. 2005, Gardelle et al. 2009*).

*1.3: The Gourma Region of Mali*

The Gourma region of Eastern Mali is located within the loop of the Niger River and extends down to the border of Burkina Faso, covering the entire climatic gradient of the Sahel [*Figure 1.5*]**.** Like elsewhere in the Sahel, the Gourma has only one rainy season between June and September that is followed by a long dry season of 7-8 months in the South and 9-10 months in the North. The same severe droughts of the 1960s and 1980s that plagued much of the Sahel also plagued the Gourma, but a return of average rains since the 1990s has been recorded (*Mougin et al. 2009, Frappart et al. 2009*).
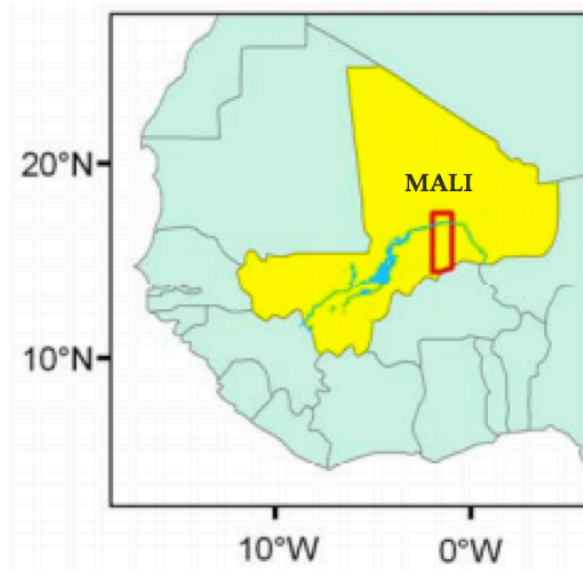
*Figure 1.5: The Gourma region of Mali (adapted from Mougin et al. 2009)*

Like much of the Sahel, annual grasses dominate much of the landscape in the Gourma. However, thickets of woody shrubs and trees called 'tiger bush' can form along drainage lines, in temporary pools, in depressions, and in shallow soils—although populations were decimated by the Great Sahelian Drought (*Hiernaux and Gerard 1999, Hiernaux et al. 2008*). Cultivated land is sparse, covering only a few percent of the land, and is concentrated in the Southern Gourma (*Mougin et al. 2009*).

The Gourma region, like Niamey, is endorheic, contributing and receiving little water from the nearby Niger River. Sandy soils comprise the majority of the region (58 percent), shallow soils on rock and hardpan outcrops (30 percent) and fine textured soils in the low land areas (12 percent) make up the rest (*Gardelle et al. 2009*). Runoff from the sandy soils on dune slopes is negligible compared to the structured system of rills fed by the shallow and low land soils. Concentrated surface runoff ends in one or several often interconnected temporary ponds that flood in the wet season and evaporate completely in

7

the dry season. As in other areas of the Sahel following the Great Sahelian Drought, surface runoff due to woody vegetation die-off and soil erosion has caused many ephemeral ponds to become perennial (Mougin et al. 2009, Gardelle et al. 2009).

*1.4: Study Site: Agoufou Pond*

The focus of this study is Agoufou, a previously ephemeral pond in the central Malian Gourma that has seen an astounding increase in volume since the Great Sahelian Drought. Agoufou pond had been ephemeral for many years prior to the Great Sahelian Drought as witnessed by maps, satellite imagery, and the presence of large dead trees in the center of the pond. These trees (e.g Anogeisus leiocarpus and Acacia nilotica) are adapted to life in ephemeral pools, but will die if inundated year-round. They existed in the 1950s as evidenced by aerial imagery, so it is known that Agoufou must have been ephemeral even during the wet period of the mid-20th century [*Figure 1.6*] (*Gardelle et al. 2009*).
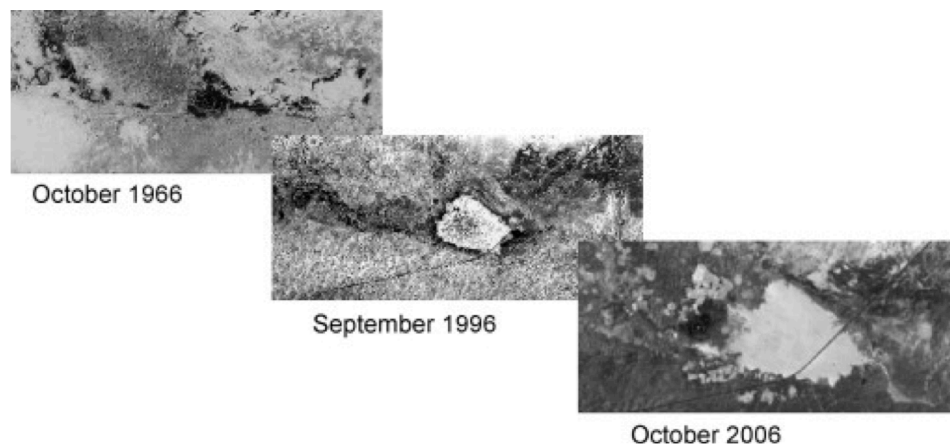


*Figure 1.6: Agoufou lake expansion over time (adapted from Gardelle et al. 2009)*

The Agoufou basin spans 265 square kilometers. Sixty five percent of basin area is covered by stabilized and active sand dunes covered in annual grasses, characterized by high infiltration rates and low surface runoff. The other 35 percent consists of hardpan covered sporadically by sand lenses, characterized by low infiltration rates and high surface runoff (*Kaptue et al., personal communication*). Woody vegetation exists primarily within riparian zones [*Figure 1.7*]**.**

Historically, a lack of perennial water sources in the region limited settlement, and only seasonal grazing was commonplace.  However, since Agoufou has become perennial, a small village has formed in the area and 5-10 thousand cattle now reside in there year round. Previously transhumant pastoralists have settled and begun agro-pastoral lifestyles, growing millet in addition to their pastoral activities (*Anecdotal data and Google Earth*).
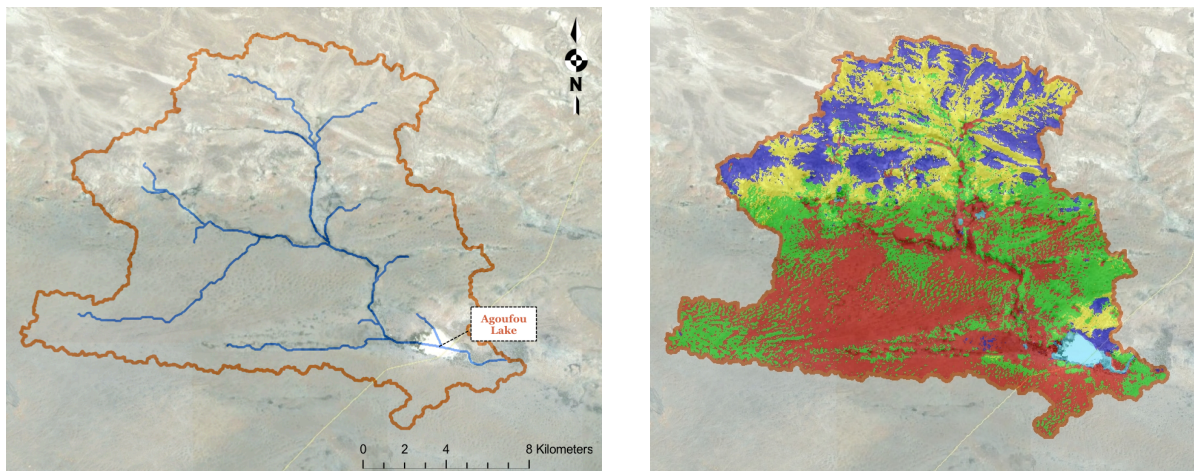


*Figure 1.7: Left: Agoufou basin extent and DEM-delineated stream network. Right: Land cover classes [Green: active dunes/developing savannah; Red: stabilized dunes/developed savannah, Yellow: sand lenses on hardpan/degraded savannah, Blue: hardpan/mostly bare with some shrubs; Light Blue: open water]*

## 2. Project Overview & Objectives

*2.1: Project Overview—Coupled Human and Natural Systems*

Following the Great Sahelian Drought of the mid 1980s, an eco-hydrologic regime shift occurred in many areas of the Sahel. Previously ephemeral ponds have become perennial in the Gourma of the Malian Sahel (*Gardelle et al. 2009*). We hypothesize that this system-level "paradoxical" regime shift was due to woody vegetation die-off during the drought and subsequent erosion of the soil that it once held in place. Erosion of the sand lenses above hardpan in the Gourma has allowed for increased surface runoff, leading to increased volumes in ponds such that they do not completely evaporate in the dry season. In recent years, the ponds have continued to increase in size without a concomitant increase in annual precipitation, leading us to believe that the system has not yet reached an equilibrium state.

With the return of the rains following the Great Sahelian Drought, it would be anticipated that some, if not all woody vegetation would begin to return. In response, surface runoff would decrease and the ponds could have returned to their ephemeral state. However, because a surface water source exists year round, some historically transhumant pastoralists have responded by settling permanently near these ponds. Year round grazing and an increase in tilling of land for agriculture may be limiting the ability of vegetation to return, keeping the system from returning to its original state. We hypothesize that continuous agro-pastoral activities may now maintain vegetation degradation in these basins. Thus, it is no longer sufficient to study just eco-hydrologic responses in the basin when it has become a coupled, socio-eco-hydrologic system.

*2.2 General Project Objectives*

The main focus of this project is to explore the new socio-eco-hydrologic system that has developed in the Malian Sahel—the interactions and feedbacks resulting from human decision-making in a changing landscape and their effect on hydrologic response, land cover, and livelihoods. System response is largely dependent on basin geomorphology, as similar eco-hydrologic responses following the Great Sahelian Drought were seen in the Niamey region of Niger, but a lake state change did not occur there and therefore no social reorganization has followed. This difference is due to high rates of deep drainage to a hydraulically connected and rising aquifer in Niamey, whereas in the Gourma region the underlying impermeable continental terminal limits deep drainage and allows for ponding. Questions of whether the response of this system is elastic or plastic in response to eco-hydrologic processes following the Great Sahelian Drought will be addressed.

To completely understand how and why the natural socio-eco-hydrologic system in the Gourma seemingly switched to an alternate stable state following the Great Sahelian Drought, knowledge of the rainfall-vegetation cycle, basin geomorphology, and agro-pastoral community response to changes in their landscape must all be taken into account simultaneously. These systems are linked, and as such must not be modeled as independent. If our project hypothesis stated above is proven to be correct, the interactions and feedbacks of the Sahelian socio-eco-hydrologic system may have implications for dryland pastoral systems worldwide. The methodology proposed to assess the project hypothesis are as follows:

A. *Detailed process-oriented historical, socioeconomic, and eco-hydrologic field studies in the primary watershed (Gourma, Mali) will inform process-based coupled socio-eco-*

*hydrologic modeling exercises. The coupled model will consist of SWAT as the hydrologic component, a vegetation dynamics sub-model, and a rule-based pastoral human decision-making sub-model.*

B. *Sahelian pond case studies—find and assess the likely causes of other system state changes and their causes in different regions of the Sahel following the Great Sahelian Drought*

C. *Assess the potential for other future lake state changes of other regions of the Sahel*

As will be discussed later in this paper, detailed field studies in the primary watershed (*Methodology A*) were unable to be completed due to unforeseen reasons. As such, remotely sensed data, previous studies in the region, and even anecdotal information were used to parameterize the models. As the project has evolved, a new objective has understandably revealed itself:

D. *Address the difficulty of modeling efforts in ungauged basins with uncertainty analysis and unique parameterization/calibration*


*2.3: Specific Project Objectives*

This paper will focus on the process-based hydrologic modeling effort and the challenges involved with parameterizing and calibrating a hydrologic model in an ungauged basin with minimal data. It will not discuss methods, results, or conclusions from the socio-eco-hydrological model coupling effort (*General Methodology A*). The methodologies of this paper are as follows:

A. *Gather all applicable data possible to parameterize hydrologic model (including from nontraditional sources)*

B.  *Perform uncertainty and sensitivity analysis of hydrologic model parameters*

C.  *Calibrate hydrologic model prior to model coupling*

D.  *Preliminarily test general project hypotheses with uncoupled model*

## 3. Methods

*3.1: The Soil and Water Assessment Tool (SWAT) 2009*

The Soil & Water Assessment Tool (SWAT) is a semi-distributed basin-scale model developed for the U.S. Department of Agriculture Agricultural Research Service by Blackland Research Center at Texas A&M University. SWAT was designed to predict the impact of land management practices on water, sediment, and non-point source pollution yields in large, complex watersheds [*Neitsch et al. 2011*]. SWAT is a continuous time model that operates on a daily time step. In SWAT, the basin area is divided into multiple spatially defined subbasins based on watershed delineation from a digital elevation model (DEM) using a geographic information system (GIS) [*Figure 3.1*]. Each subbasin is further subdivided into aspatial Hydrologic Response Units (HRUs), each of which is composed of a set of disconnected subareas with similar characteristics based on land-use, soil, and slope classes. If desired for improved computational efficiency, the user has the ability to limit the number of HRUs in a subbasin by neglecting those that contribute a negligible amount to subbasin area. The response of each HRU is calculated and summed at the subbasin level and routed downstream. The water balance is simulated at the HRU level for four different storage volumes: soil profile, shallow aquifer, deep aquifer, and small lake.

*Figure 3.1*: SWAT DEM-delineated Subbasins for Agoufou basin

SWAT has the ability to predict the movement of pesticides, sediments, and other nutrients throughout the system. Surface runoff is calculated using a modified Soil Conservation Service (SCS) Curve Number approach or the Green & Ampt infiltration method; however, the Green & Ampt method requires at least hourly precipitation data. SWAT incorporates a kinematic storage model for subsurface flow developed by Sloan et al. 2003: the model simulates subsurface flow in a two-dimensional cross-section along a flow path down a hillslope. The user can choose between two different channel routing methods: variable storage routing or Muskingum River routing—both are variations of the kinematic wave model. Evapotranspiration and climate will be discussed in the following sections. SWAT also utilizes a simplified version of the Environmental Policy Integrated Climate (EPIC) plant growth model, which simulates plant development based on daily-accumulated heat units, potential biomass based on a method developed by Monteith, and growth inhibited by temperature, water, nitrogen and phosphorous stresses (*Williams 1995)*. Management options including planting, harvest, irrigation, application of pesticides

15

and fertilizers, and grazing can also be scheduled at different times during the simulation. In ponds and lakes inside the watershed, algal and bacterial growth can also be simulated. The basic model command loop is described in *Figure 3.2* below.
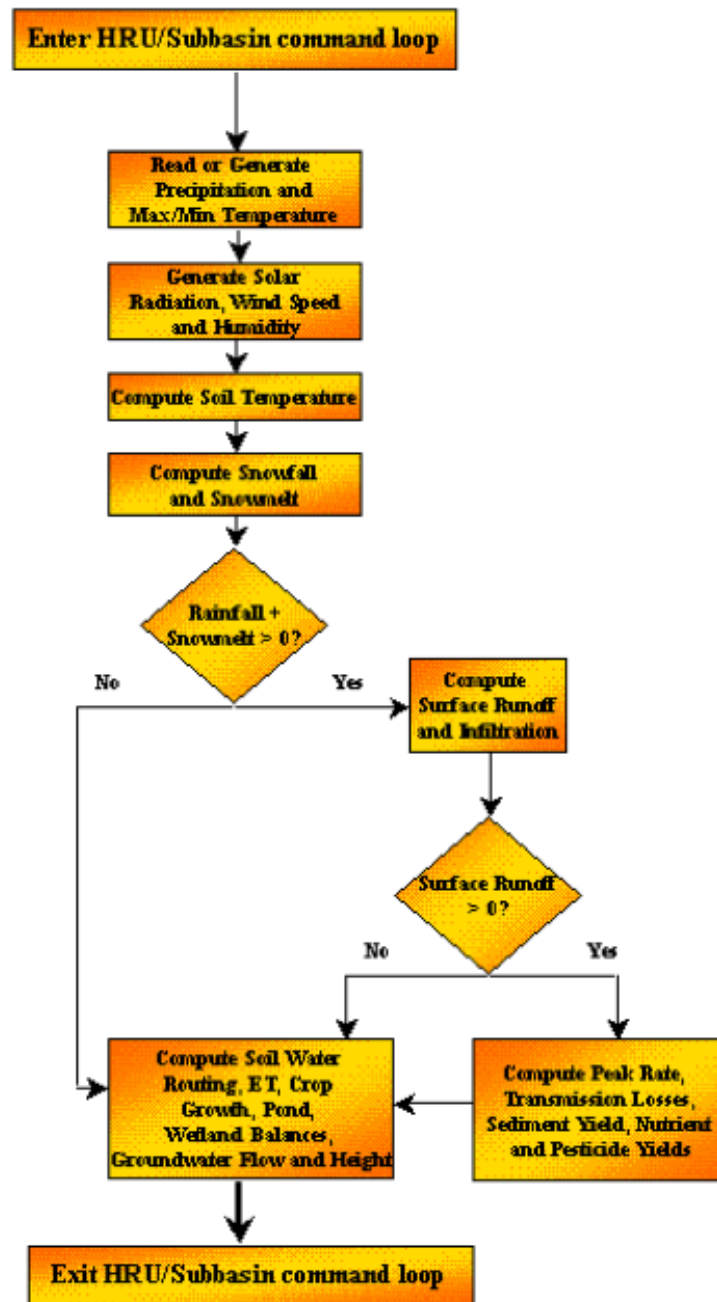


*Figure 3.2*: SWAT model command loop (Nietsch et al. 2011)

*3.2: Modification of SWAT Evapotranspiration Calculation*

SWAT has the ability to calculate potential evapotranspiration (ET$_p$) in 3 different ways: Penman-Monteith [*Monteith, 1965*], Priestley and Taylor [*Priestley and Taylor, 1972*], and Hargreaves and Samani [*Hargreaves et al. 1982*]. ET$_p$ is defined as the evapotranspiration that would occur from a moist surface under current atmospheric conditions, limited only by the amount of energy that is available at the land surface interface. Actual evapotranspiration (ET$_a$) is then calculated as a function of ET$_p$ and available water on the surface and in the soil column.

A simple modification was made to the SWAT model to include the complementary relationship for evapotranspiration. The complementary relationship states that there exists a complementary feedback mechanism between actual and potential evapotranspiration [*Bouchet, 1963, Morton 1983*], i.e. the two rates are not independent of each other. Interactions between ET$_p$ and ET$_a$ rates are established based on the degree of saturation of the soil as opposed to only atmospheric demand for water vapor. In addition, the effect that evapotranspiration has on the energy budget at the land surface must be taken into account [*Hobbins et al. 2001*]. Under conditions where actual evapotranspiration and potential evapotranspiration are equal, this rate is referred to as wet environment evapotranspiration (ET$_w$), i.e. when atmospheric demand is fully met by supply of water at the surface. The general complementary relationship [*Figure 3.3*] is then expressed as:

$$(Eq.3.1) \qquad ET_a + ET_p = 2 \cdot ET_w.$$
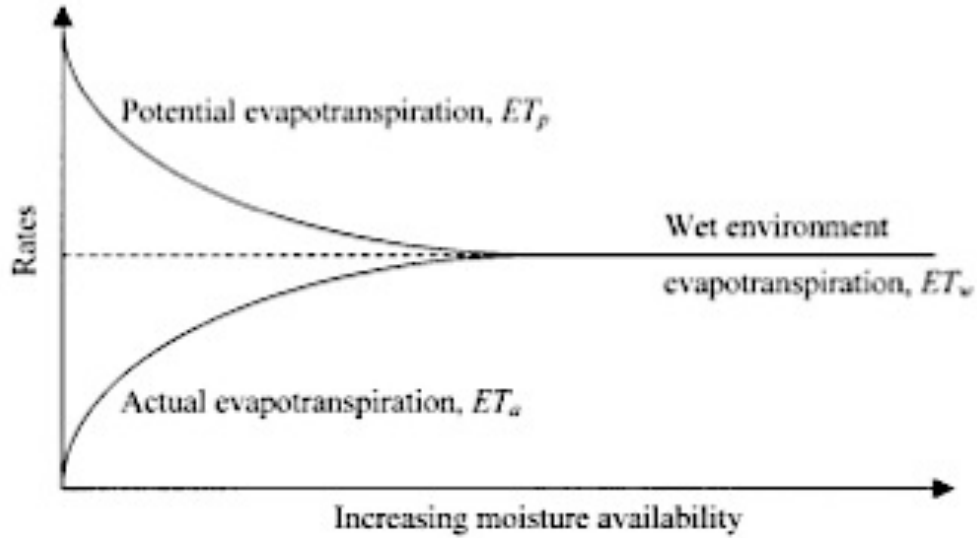
*Figure 3.3*: The complementary relationship for evapotranspiration (*Hobbins et al. 2001*)

The Advection Aridity (AA) model (*Brutsaert and Stricker, 1979*) for the complementary relationship was used for this paper. The AA model utilizes the Penman (or Penman-Monteith) expression for potential evaporation, $ET_p$:

$$(Eq.\,3.2) \qquad ET_p = \frac{Q_n}{L_v}\left(\frac{\Delta}{\Delta + \gamma}\right) + \left(\frac{\Delta + \gamma}{\Delta}\right)E_A.$$

The first term represents energy budget considerations and the second term represents the effects of advection. Here $Q_n$ is the net available energy available at the land surface, $L_v$ represents the latent heat of vaporization, $\Delta$ is the slope of the saturated vapor pressure curve at the current air temperature, $\gamma$ is the psychrometric constant, and $E_A$ represents the drying power of the air. The drying power of air is a function of wind speed ($U_z$) at elevation Z above the surface and the difference between the saturation vapor pressure ($e_{s,a}$) and vapor pressure ($e_a$) of the air:

$$(Eq.\,3.3) \qquad E_A = f(U_z)(e_{s,a} - e_a).$$

The AA model uses an empirically based approach for the wind function, $f(U_z)$, proposed by (*Penman, 1948*):

$$(Eq.\,3.4) \qquad f(U_z) \cong f(U_2) = 0.26(1 + 0.54 U_2)\eta.$$

Here $U_2$ represents wind speed in m·s$^{-1}$ measured at 2-m above the evaporation surface, and vapor pressures measured in hPa to yield $E_A$ in mm·d$^{-1}$. $\eta$ is required to convert $E_A$ to the proper SI units.

To calculate wet environment evapotranspiration, $ET_w$, the AA model uses the partial equilibrium evapotranspiration equation from (*Priestley and Taylor 1972*):

$$(Eq.\,3.5) \qquad ET_w = \frac{Q_n}{L_v}\left(\frac{\Delta}{\Delta + \gamma}\right)\alpha.$$

Here the value of $\alpha$ is a constant equal to 1.28. Finally, we can obtain a closed form solution for actual evapotranspiration, $ET_a$, using the Advection Aridity (AA) model for the Complementary Relationship:

$$(Eq.\,3.6) \qquad ET_a = (2\alpha - 1)\left(\frac{Q_n}{L_v}\right)\left(\frac{\Delta}{\Delta + \gamma}\right) - \left(\frac{\Delta + \gamma}{\Delta}\right)E_A.$$

*3.3: SWAT Weather Generator Preparation*

SWAT is driven by daily values of precipitation, maximum and minimum temperature, solar radiation, relative humidity, and wind speed. If the data exists for the entire simulation period, then the user has the ability to read in these inputs from an external file. However, if there are gaps in the data or if the data does not cover the entire desired simulation period, SWAT includes the weather generator WXGEN (*Sharpley and Williams, 1990*) to generate daily climatic data. Preferably, at least 20 years of records should be used to calculate the necessary statistics for WXGEN to run adequately.

The following parameters are required by the weather generator for each month: mean daily maximum temperature, mean daily minimum temperature, standard deviation of daily maximum temperature, standard deviation of daily minimum temperature, mean total monthly precipitation, standard deviation of daily precipitation, skew coefficient of daily precipitation, probability of a wet day following a dry day, probability of a wet day following a wet day, mean number of wet days, maximum ½ hour rainfall in entire period of record, mean daily solar radiation, mean daily dew point temperature, and mean daily wind speed.

For this paper, wind speed, relative humidity, solar radiation and minimum and maximum temperature are generated. Daily precipitation events were produced independently (*See Section 3.5*). WXGEN was parameterized using a combination of global, regional, and local datasets (*Climatic Research Unit (CRU) TS 2.1, NASA Surface Meteorology and Solar Energy, National Climatic Data Center (NCDC), Hombori Gauge Data, AMMA gauge data*)—although some of the local gauge data was deemed unreliable due to gaps and anomalous values.

Minimum temperature, maximum temperature, and wind statistics required by WXGEN were derived by computing each statistic from the daily data available from Hombori and AMMA gauge data, and compared to monthly averages from CRU, NASA Surface Meteorology and the NCDC. The long-term simulated mean minimum and maximum monthly temperatures were within ±3° Celsius of average regional data from the combined CRU, NASA, and NCDC datasets. Relative humidity and solar radiation statistics were only available through CRU and NASA, and for the most part did not deviate much from each other. The mean value of the two datasets was used for WXGEN.

The watershed of interest, Agoufou basin, located in the Gourma of Northern Mali, is rather small, spanning only 265 square kilometers. In addition, the only global soil and vegetation datasets found were quite coarse, with grid sizes of 1 kilometer and 500 meters, respectively. Therefore, the spatial heterogeneity of the vegetation and soils in the basin is not represented adequately by these datasets (*Figure 3.4*).
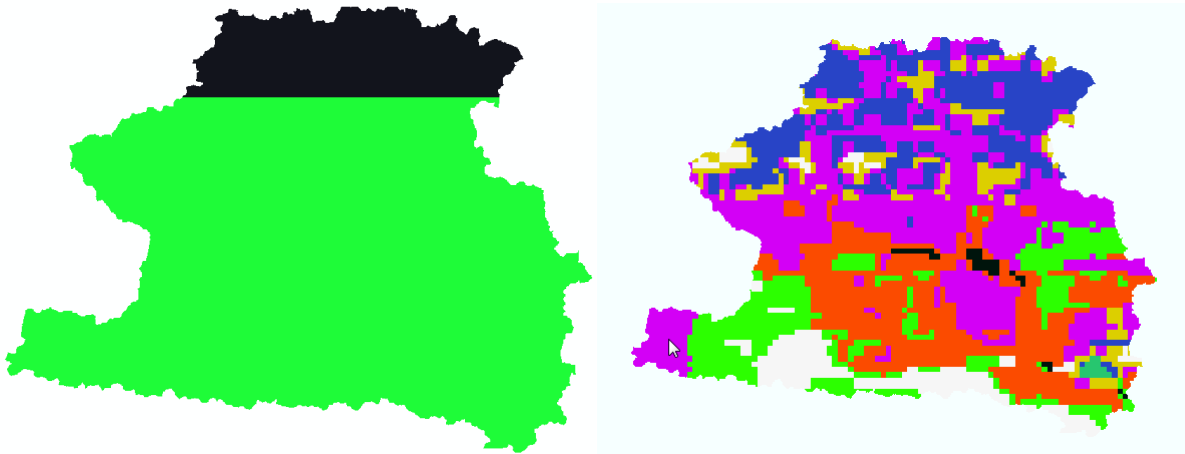


*Figure 3.4*: Coarse soil (left) and vegetation (right) datasets for SWAT simulation [Different colors represent different classes of soils (left) and vegetation (right). This level of spatial heterogeneity was deemed inadequate.]

To address this issue, we used a 30-meter vegetation map derived from LANDSAT imagery (*Kaptue et al., personal communication*). The analysis of the LANDSAT imagery over Agoufou basin revealed five major land cover types [*Figure 3.5*]**:** (1) open water, (2) hardpan, (3) degraded savannah on sand lenses covering hardpan, (4) developing savannah, and (5) fully developed savannah. Each land cover type was linked to a vegetation class in the SWAT database [*Table 3.1*], and then modified to resemble what

exists in Agoufou [*Table 3.2*]. Special care was taken to ensure that the most sensitive vegetation parameters in SWAT were as accurate as possible (*See Section 3.6*).

As for the soil map, since the one-kilometer grid of two soils classes did not provide enough information and did not fit expectations given the high-resolution vegetation map [*Figure 3.5*], it was assumed that four major classes of soils exist. Each soil class was assumed to match with a corresponding vegetation class from the high-resolution vegetation map: (1) impervious clay soils (hardpan) lie underneath open water and align with the aforementioned hardpan vegetation class, (2) shallow sand lenses align with the degraded savannah vegetation class, (3) very deep sand with some active dunes aligns with the developing savannah vegetation class, and (4) deep sand with stabilized dunes aligns with the fully-developed savannah vegetation class. Numerical ranges for the most sensitive parameters for these soil classes (*See Section 3.*6) were derived from multiple sources [*Table 3.3*] (*AMMA-Catch, HAPEX-Sahel, Geeves et al. 2007a, Kaptue et al. 2010, Harmonized World Soil Database*). Although this is by no means a perfect solution, the representation of the spatial heterogeneity of the region was increased by a large magnitude thus allowing a more detailed simulation of the basin.
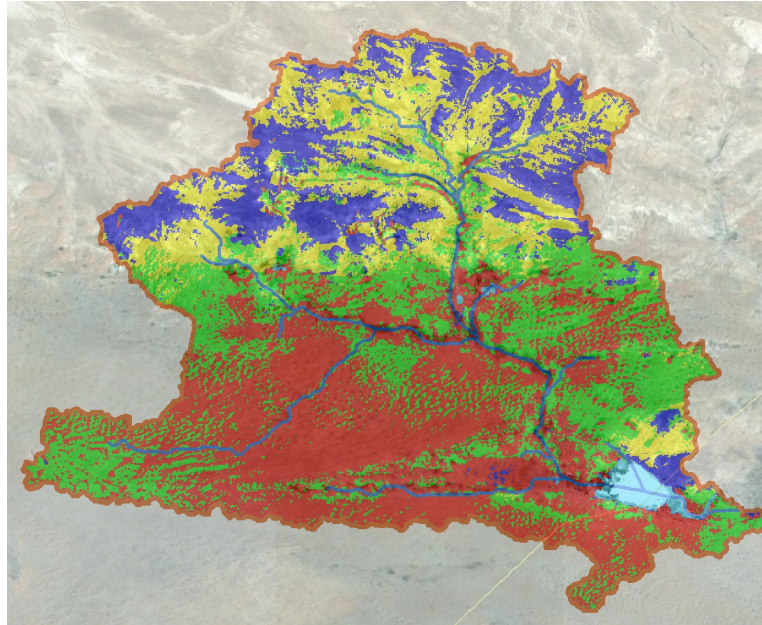
*Figure 3.5*: Vegetation raster & proxy for soils *[Green: active dunes/developing savannah; Red: stabilized dunes/developed savannah, Yellow: sand lenses on hardpan/degraded savannah, Blue: hardpan/mostly bare with some shrubs; Light Blue: open water]*

*Table 3.1*: Land cover classes linked to SWAT vegetation classes

| Land Cover Classes: | SWAT Vegetation Class: |
|---|---|
| DEEP SAND AND SOME ACTIVE DUNES [Developing savannah] | Range-Brush |
| STABILIZED DUNES [Developed savannah] | Range-Grass |
| SAND LENSES ON HARD PAN [Degraded savannah] | Range-Brush |
| HARDPAN [mostly bare with sparse shrubs] | Southwestern US (Arid) Range |
| OPEN WATER | Water |

*Table 3.2*: Sensitive vegetation parameters in SWAT

| Sensitive Vegetation Parameters in SWAT: | | Physically acceptable parameter ranges for each Land Cover class: | | | |
|---|---|---|---|---|---|
| Parameter Name: | Parameter Description: | DEEP SAND AND SOME ACTIVE DUNES [Developing savannah] | STABILIZED DUNES [Developed savannah] | SAND LENSES ON HARD PAN [Degraded savannah] | HARDPAN [mostly bare with sparse shrubs] |
| IDC | Land Cover/Plant Classification | Warm season annual | Warm season annual | Warm season annual | Warm season annual |
| BLAI ($m^2 m^{-2}$) | Maximum Leaf Area Index | [1-2] | [1.5-2.5] | [1-2] | [0-0.5] |
| ALAI_MIN ($m^2 m^{-2}$) | Minimum Leaf Area Index | 0 | 0 | 0 | 0 |
| CN2 | SCS Curve Number for Moisture Condition #2 | [40-60] | [30-50] | [55-80] | [65-90] |
| OV_N | Manning's n for Overland Flow | [0.15-0.2] | [0.2-0.25] | [0.1-0.15] | [0.05-0.1] |

*Table 3.3*: Sensitive soil parameters in SWAT

| Sensitive Soil Parameters in SWAT: | | Physically acceptable parameter ranges for each Land Cover class: | | | |
|---|---|---|---|---|---|
| Parameter Name: | Parameter Description: | DEEP SAND AND SOME ACTIVE DUNES [Developing savannah] | STABILIZED DUNES [Developed savannah] | SAND LENSES ON HARD PAN [Degraded savannah] | HARDPAN [mostly bare with sparse shrubs] |
| SOL_Z (m) | Depth of Layer | [2-4] | [1.5-3] | [0-0.3] | 0 |
| SOL_K ($mm hr^{-1}$) | Hydraulic Conductivity | [100-300] (sand) | [60-150] (loam/sandy-loam) | [5-70] (clay/clay-loam) | 0 |
| SOL_AWC ($mm H_2O mm^{-1} soil$) | Plant Available Water Capacity | [0.1-0.15] | [0.15-0.2] | [0.5-0.1] | 0 |
| SOL_ALB | Moist Soil Albedo | [0.19-0.21] | [0.21-0.23] | [0.15-0.17] | [0.09-0.11] |
| SOL_BD ($g cm^{-3}$) | Moist Soil Bulk Density | [1.5-1.65] (sand) | [1.25-1.7] (loam/sandy-loam) | [1.2-1.55] (clay/clay-loam) | [1.2-1.4] (clay) |
| CLAY (%) | Clay Content | ≈5 | ≈13 | ≈22 | ≈19 |
| SAND (%) | Sand Content | ≈90 | ≈66 | ≈42 | ≈47 |
| SILT (%) | Silt Content | ≈5 | ≈21 | ≈36 | ≈34 |
| ROCK (%) | Rock Content | ≈4 | ≈4 | ≈5 | ≈27 |

*3.5: Temporal Precipitation Downscaling*

Because SWAT requires daily precipitation data, and no such data exists for the desired modeling period, a method to produce the required daily data was necessary. While SWAT's WXGEN can produce daily precipitation for the user, we wanted to have more control over the process because it is one of the most important drivers of hydrologic response. It was also necessary to produce monthly precipitation totals that were identical to those used by the dynamic vegetation model that SWAT will eventually be coupled (*see Section 2.2*) with—a task that WXGEN cannot complete.

Two datasets covering the desired simulation area were chosen to be used in precipitation downscaling: (1) the Climatic Research Unit (CRU) TS 2.1 dataset contains monthly totals of precipitation dating back to 1901 and (2) the Tropical Rainfall Measuring Mission (TRMM) dataset contains monthly precipitation statistics including storm duration, intensity, and number of storm arrivals per month dating back to 1998.

Using the TRMM dataset for each month dating back to 1998, a Poisson distribution was fit to the number of storm arrivals per month (i.e. an exponential distribution was fit to the inter-arrival times between storms):

$$(Eq.\,3.7) \qquad v_{mon} = \frac{days_{mon}}{rainy\ days_{mon}}$$

where $v_{mon}$ is the parameter of the Poisson distribution of storm arrivals per month, $days_{mon}$ is the number of days in month, and *rainy days$_{mon}$* is the mean number of rainy days per month from the TRMM dataset. In addition, a two-parameter gamma distribution was fit to storm intensities for each month using the Method of Moments.

The downscaling process is outlined in *Figure 3.6*. Firstly, the Exponential distribution is sampled to determine the amount of days until the next event. If an event occurs in the month, the gamma distribution is sampled for event intensity. This process repeats until the amount of days until the next event exceeds the number of days left in the month. Once the downscaling process is performed for each month in the simulation, the total monthly precipitation is summed and corrected to ensure equality with the monthly totals of the CRU dataset. After this adjustment, the parameters of each distribution are recalculated to confirm that the synthetic precipitation has conformed to the specifications of each distribution.
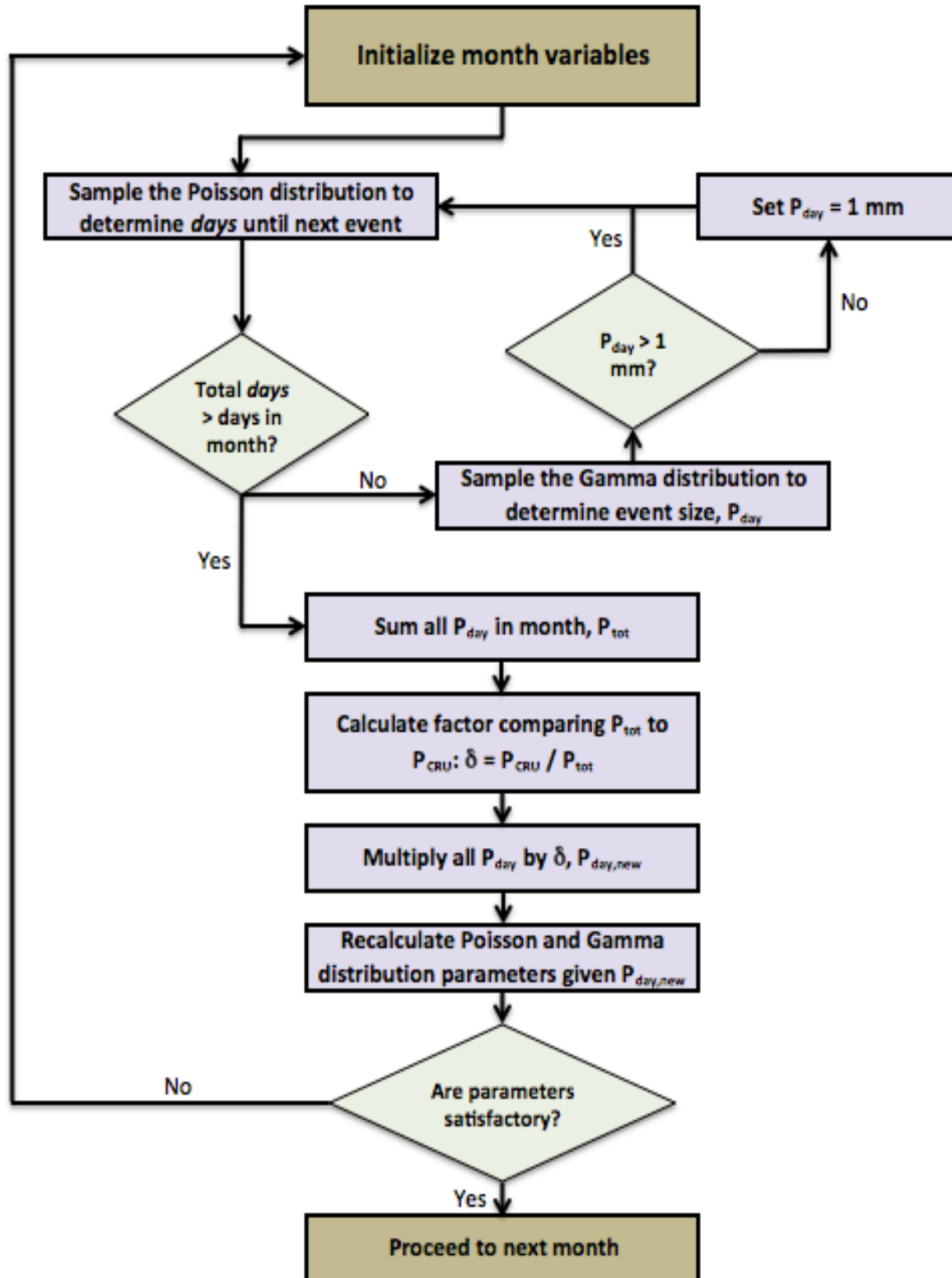
*Figure 3.6*: Precipitation downscaling schematic

*3.6: SWAT Parameter Sensitivity Analysis*

As stated in Section 1, in the Sahel, measurement stations are scarce and reliable data is often difficult to obtain. It is common for drainage basins throughout many parts of the Sahel to be ungauged or poorly gauged. Conventional hydrologic modeling techniques to calibrate and verify model parameters are rarely applicable in these cases. This problem is exacerbated when human-induced changes to the land surface and climate change impacts lead to increased uncertainty.

SWAT is a highly parameterized model, containing hundreds of parameters for the various model functions described in *Section 3.1*. In this region, data does not exist to properly utilize all the parameters and functions that SWAT provides. For this project, we are concerned only with parameters that concern the hydrologic and hydraulic functionality of the model: mainly evapotranspiration, surface and groundwater runoff, and runoff routing. The most sensitive parameters that relate to these aspects of the model were found through a rudimentary sensitivity analysis.

SWAT is a model that has been used extensively throughout the past 15 years, thus the most sensitive model parameters for purely hydrologic purposes are already known. That being said, not all parameters that are sensitive in one watershed will be sensitive in another. Of the hundreds of SWAT parameters, a Monte Carlo approach to sensitivity analysis was performed on 20 of them. SWAT was run approximately 100,000 times over a 10-year period from 2000-2010 where the majority of the LANDSAT imagery used for validation and verification (*see Section 3.7*) exists. Over the 10-year period, parameters were randomly changed within a range of physically acceptable values. An objective function relating to the volume of water in Agoufou pond was used to "score" different model runs. The Nash-Sutcliffe model efficiency metric was

used between simulated and known lake volumes at different times throughout the simulation. The objective function was simply defined as the value of 1 - Nash Sutcliffe metric. The "best" parameter set is that which minimized the objective function. Dotty plots—a projection of the model response surface defined by the currently selected model parameters and objective function—of these simulations for various model parameters can be found in *Figure 3.7*. The results of this analysis [*Table 3.4*] allowed us to focus efforts on acquiring the necessary data to ensure that the most sensitive model parameters represent the physical watershed. Each parameter in *Table 3.4* was ranked using the following simple formula:

$$(Eq.\,3.8) \qquad Sensitivity = \left| \frac{\Delta P}{\Delta V} \right|$$

where ΔP is the change in model parameter value to the expected parameter value and ΔV is the change in lake volume that resulted from the change in P.
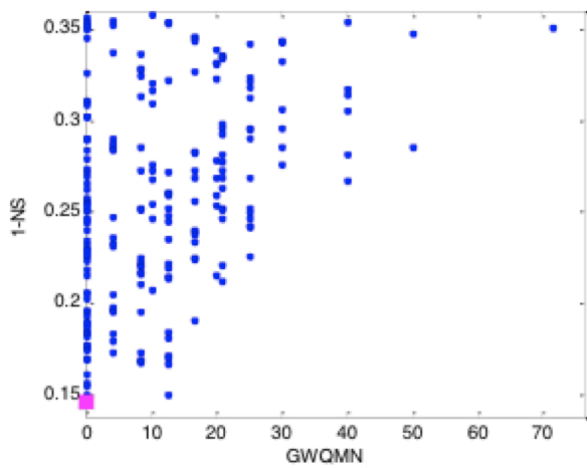


(*1*) GWQMN: Threshold water level in aquifer for baseflow to occur (mm H$_2$0)
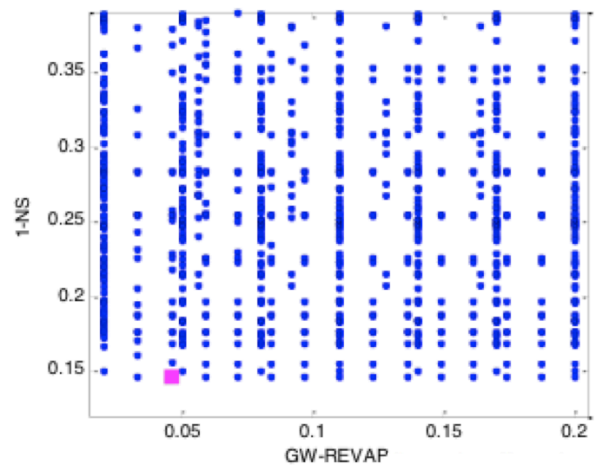
(*2*) GW-REVAP: Groundwater revap coefficient

*Figure 3.7*: Dotty Plots from sensitivity analysis of various SWAT model parameters. Vertical axis: objective function (1 - Nash Sutcliffe model efficiency metric); horizontal axis: value of model parameter used for simulation; purple square: indicator of "best" parameter value.
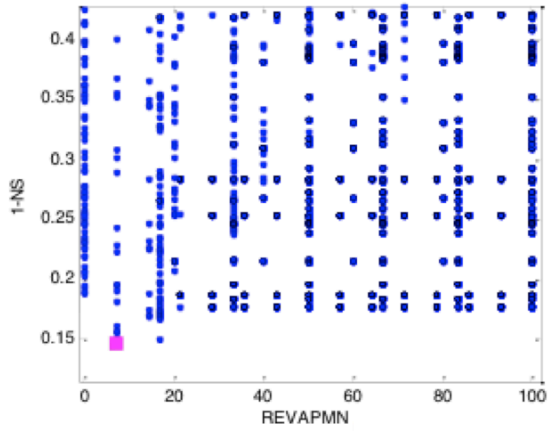
(*3*) REVAPMN: Threshold water level in shallow aquifer for revap (mm H₂0)
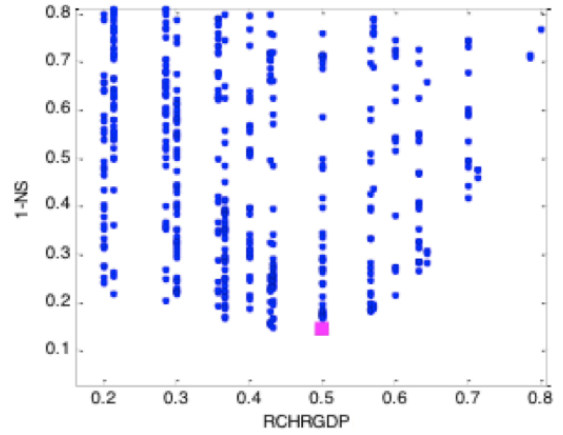


(*4*) RCHRGDP: Aquifer percolation coefficient
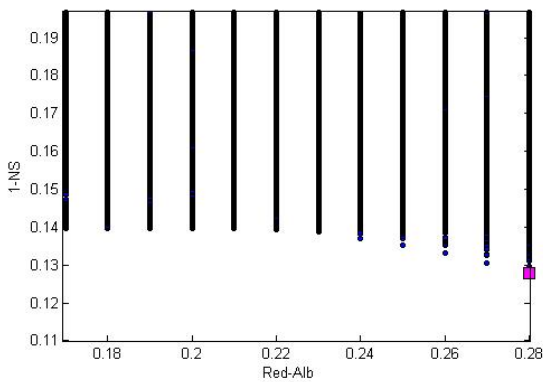


(*5*) Moist soil albedo for stabilized dunes soil class
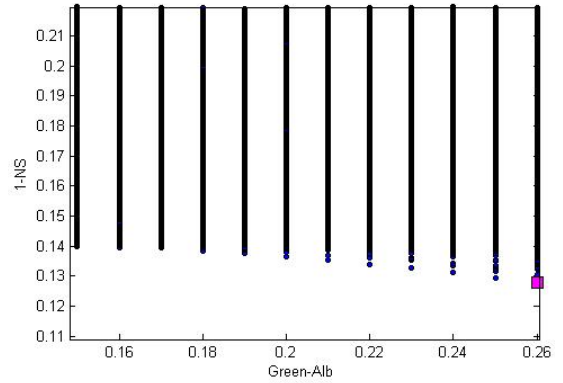


(*6*) Moist soil albedo for active dunes soil class
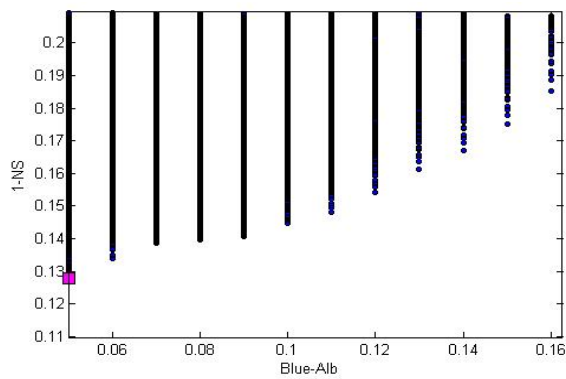


(*7*) Moist soil albedo for hardpan soil class
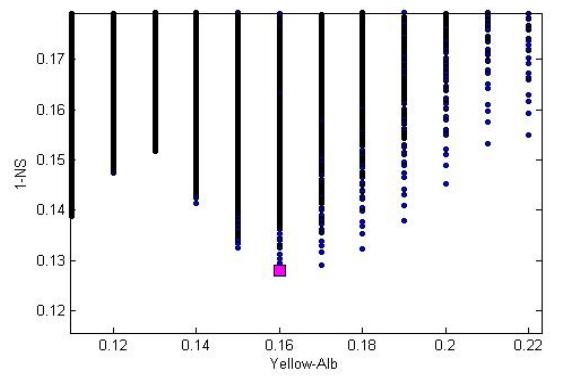


(*8*) Moist soil albedo for sand lenses over hardpan soil class

*Figure 3.7*: (continued)
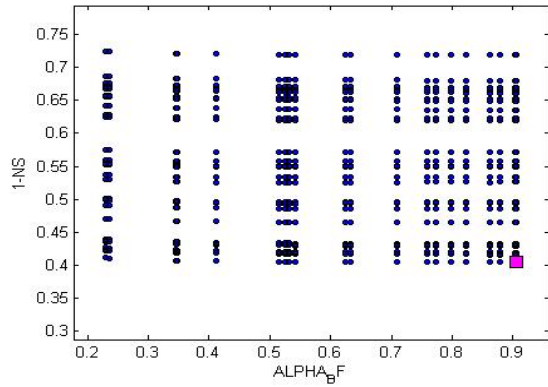
(*9*) Baseflow recession constant, α
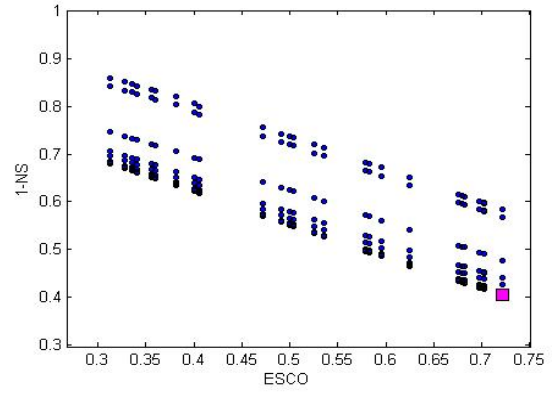


(*10*) ESCO: Soil evaporation compensation coefficient
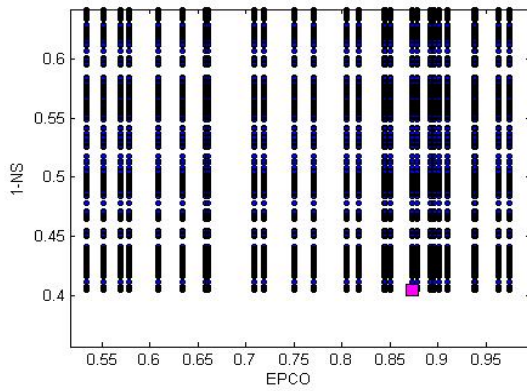


(11) EPCO: Plant uptake compensation factor
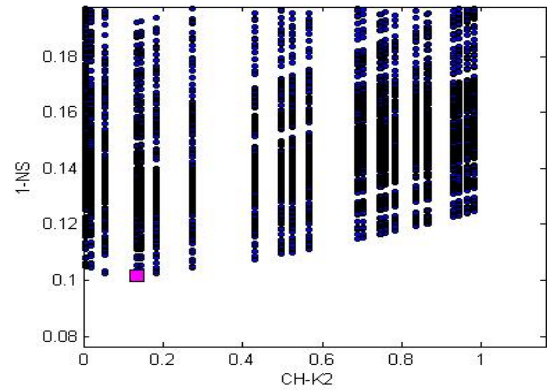


(12) Stream channel bed hydraulic conductivity
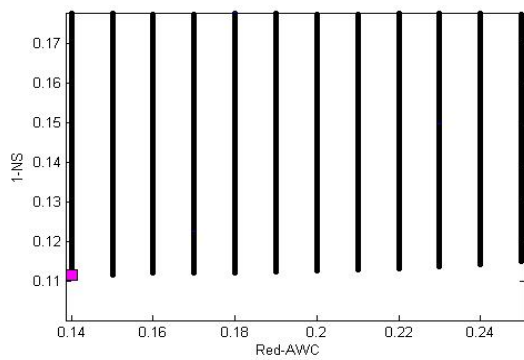


(*13*) Plant Available Water Capacity for stabilized dunes soil class
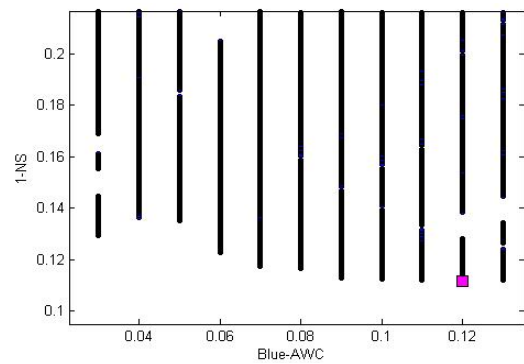


(*14*) Plant Available Water Capacity for hardpan soil class

*Figure 3.7*: (continued)
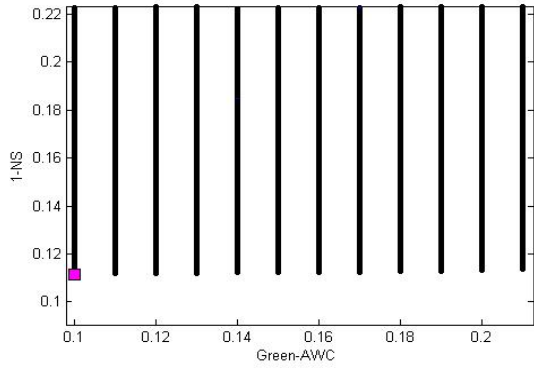
(*15*) Plant Available Water Capacity active dunes soil class
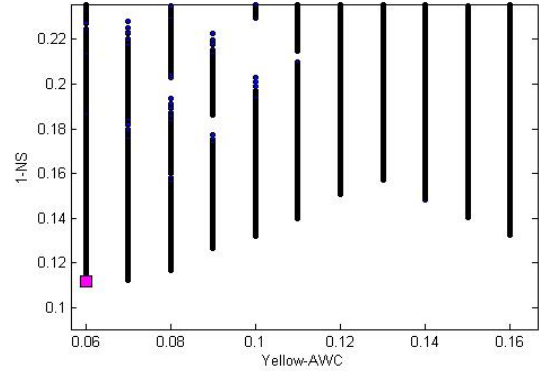


(*16*) Plant Available Water Capacity for sand lenses over hardpan soil class
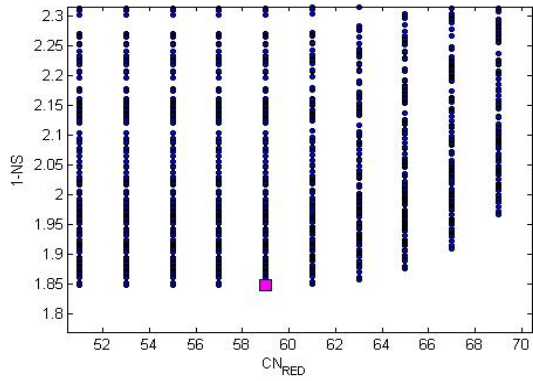


(*17*) Curve Number for stabilized dunes soil class
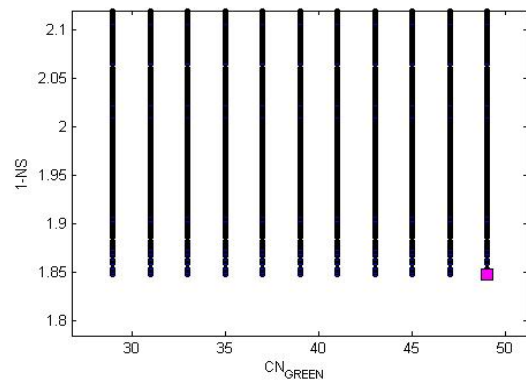


(*18*) Curve Number for active dunes soil class
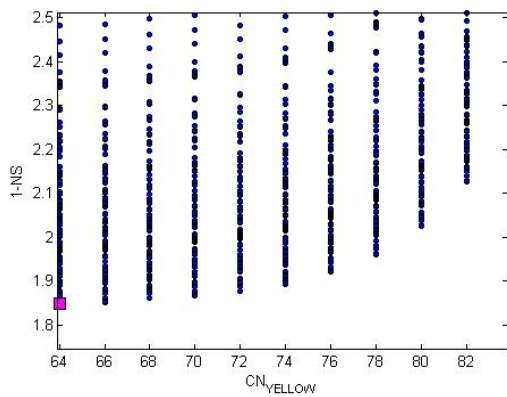


(*19*) Curve Number for sand lenses over hardpan soil class
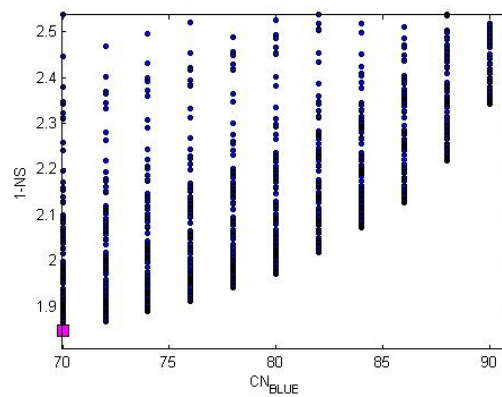


(*20*) Curve Number for hardpan soil class

*Figure 3.7*: (continued)

*Table 3.4*: Most sensitive SWAT parameters

| Most Sensitive Parameters: | | |
|---|---|---|
| *Parameter Name:* | *Parameter Description:* | *Affected Model Function:* |
| CN2 | Curve Number for Moisture Condition #2 | Surface Runoff, Infiltration, Sediment Yield |
| ESCO | Soil Evaporation Compensation Factor | Soil Evaporation |
| SOL_Z | Depth of Soil | Soil Moisture, Soil Evaporation, Percolation, |
| SOL_K | Hydraulic Conductivity of Soil | Percolation, Subsurface Flow |
| RES_K | Infiltrability of Lake Bottom | Losses of Lake Volume to Aquifer |
| RCHRGDP | Aquifer Percolation Coefficient | Losses of Soil Water to Aquifer |

| Moderately Sensitive Parameters: | | |
|---|---|---|
| *Parameter Name* | *Parameter Description* | *Affected Model Function* |
| GWQMN | Threshold water level in aquifer for baseflow | Subsurface Flow |
| SOL_ALB | Wet soil albedo | Net Radiation, Evapotranspiration, Soil Temperature |
| SOL_BD | Wet soil bulk density | Sediment Transport, Soil Temperature |
| SOL_AWC | Plant available water capacity | Plant Growth, Soil Evaporation |
| BLAI | Maximum Leaf Area Index | Plant Growth, Evapotranspiration |

*3.7: Agoufou Lake Area to Volume Relationship*

Typically hydrologic models are calibrated with streamflow data, stage measurements, soil moisture data, etc. No such data exists for Agoufou basin. To test project hypotheses with the model, it was necessary to determine some way to measure model performance, i.e. a way to calibrate and validate SWAT. To address this issue, all available LANDSAT imagery of Agoufou Lake was gathered. With these images, the areal extent of Agoufou lake was outlined numerous times dating back to the mid 1980s. While lake areas over time do not directly solve the problem, if there were a way to link pond areas to pond volumes then the model could be validated with a time series of lake volumes.

Three main methods were tested to try and find a relationship between Agoufou Lake area and volume: (1) determine elevation of lake contours using a DEM, (2) assume that the bathymetry of the lake has the same fractal (self-similar) power law relationship as the topography of the surrounding basin, and (3) compare to other shallow lakes.

Agoufou lake is quite shallow, averaging 0.5-2 meters in depth over the course of a year. A DEM with 1-meter elevation differences cannot provide the detail necessary to illustrate the differences between each lake area contour. In addition, the DEM near the lake has been shown to have many errors, possibly due to the satellite having issues with the water surface. Therefore, the DEM could not be directly used to develop the area to volume relationship using the available contours. However, the DEM was used to determine the relationship between area and volume on a larger scale in the basin [*Figure 3.8*]. Assuming that the fractal characteristics of the lake are the same as in the wider basin, then such characteristics should yield some insight into the lake area to volume relationship.

The relationship that was produced from the DEM in the larger basin was compared to that of other shallow lakes such as the Great Salt Lake, and contrasted with deeper lakes such as Lake Tahoe and Crater Lake. Obviously, these lakes were formed by different geo-physical processes, and thus have different fractal relationships. The relationship was modified slightly to ensure that the depth of the lake did not exceed 2 meters on the larger end and no less than 1/2 meter during the dry season. Armed with this relationship, a lake volume time series was constructed. The relationship is as follows:

$$(Eq. 3.8) \qquad V = 0.206 \cdot A^{1.068}$$
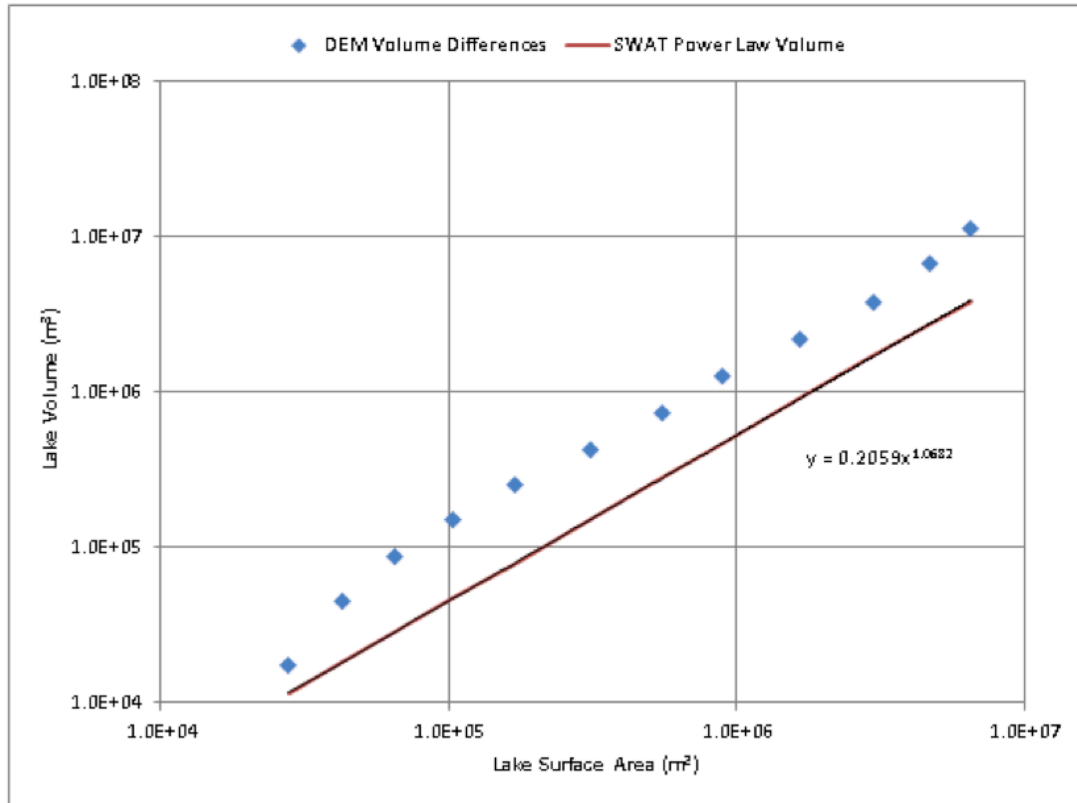
*Figure 3.8*: Area vs. Volume for Agoufou Basin

*3.8: Simulation of Convective Storm Systems – Spatial Precipitation Downscaling*

As stated in Section 1, the predominant rainfall mechanisms in the Sahel are high-intensity convective storm systems whose characteristic areal extent is smaller than the Agoufou basin. Therefore, distributing rainfall uniformly over the entire basin is not appropriate. To provide a more realistic distribution of precipitation, different synthetic daily precipitation (*See Section 3.5*) was produced for each SWAT subbasin. While the monthly total precipitation of each subbasin is the same, storms occur on different days, with different intensities and durations. [*Figure 3.9*]

35
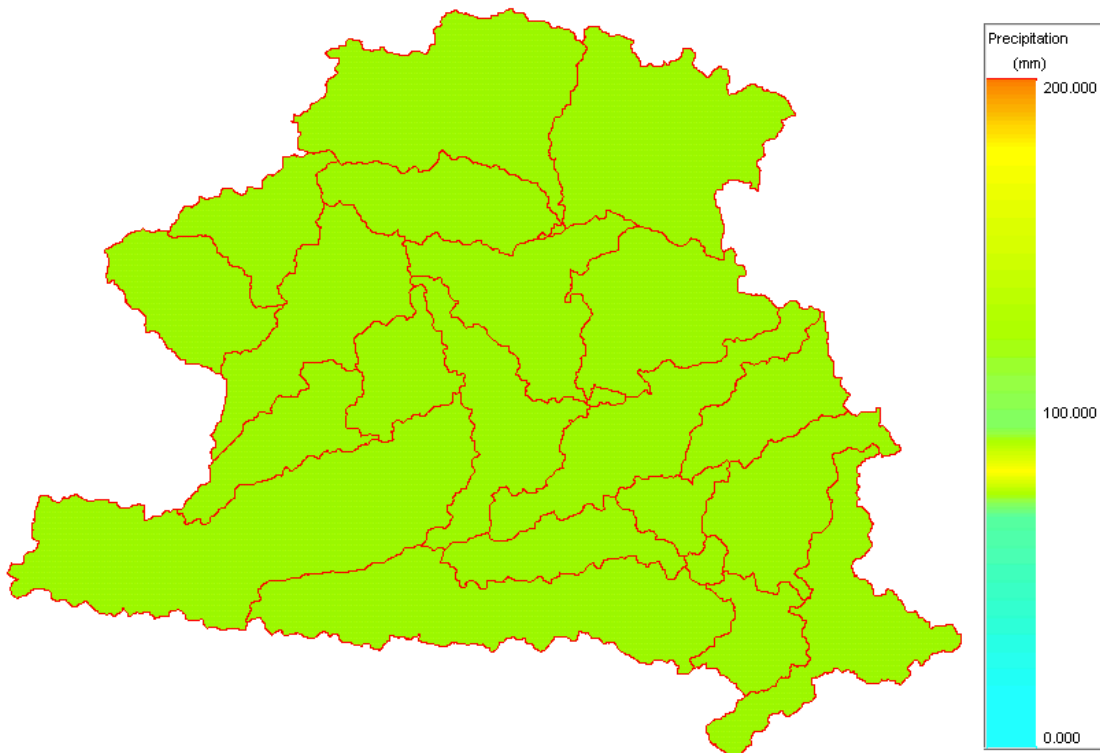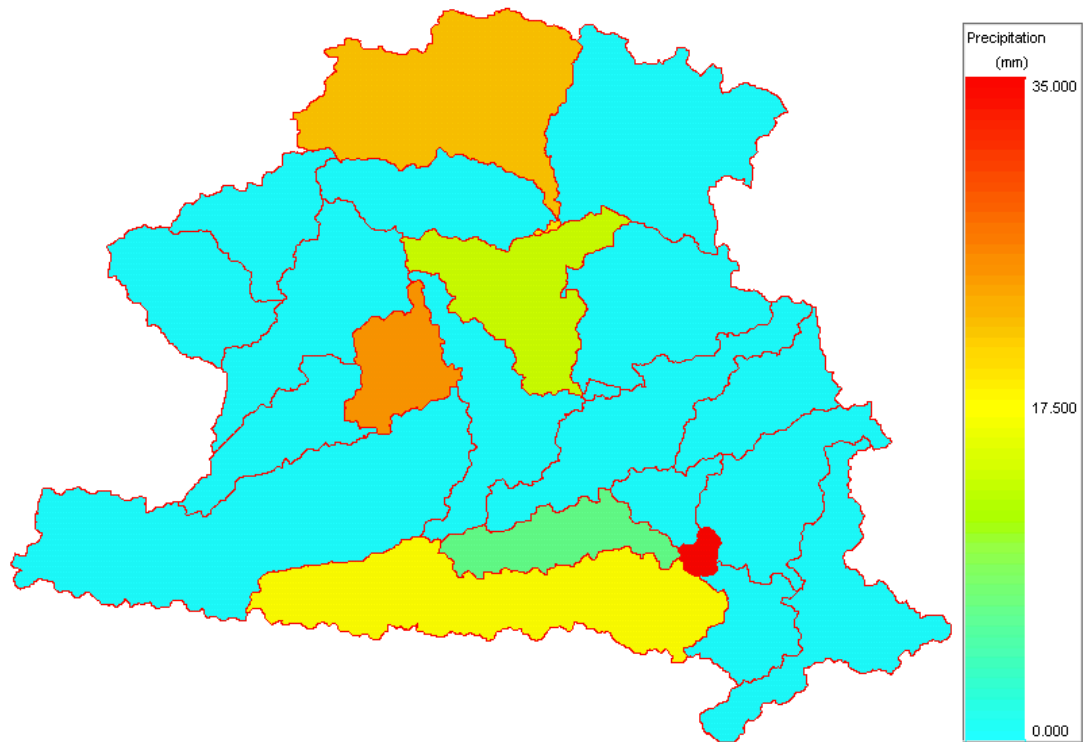
*Figure 3.9*: Spatial variability of simulated daily precipitation. Top: daily precipitation for August 24th, 1992; bottom: sum of daily precipitation for August, 1992.

## 4. Results & Discussion

*4.1: Preliminary Calibration of SWAT with Local Rain Gauge Data*

Prior to the construction of a long-term, spatially-distributed precipitation time series (*Sections 3.5 & 3.8*), the most reliable precipitation data available to run SWAT for the Agoufou basin came from a measurement station of the African Monsoon Multidisciplinary Analysis (AMMA) project, located approximately three kilometers to the southwest of Agoufou Lake. Four years of continuous hourly rainfall data exist from this station for 2002-2006 [*Figure 4.1*]. With rain gauge data at this proximity to Agoufou basin, one should expect a higher level of accuracy in model predictions of water volumes than with regional data. Rain gauge data also exists dating back to 1984 from the small town of Hombori, approximately 22 kilometers west of Agoufou Lake. Unfortunately, this data was found to be essentially useless. Large gaps exist (entire months) and annual sums are far below the regional average. Therefore, in terms of rain gage data in the area, the few years of data from the AMMA station are all that are available. For these four years, precipitation was distributed uniformly over the entire watershed, unlike what is shown in *section 3.8* for long-term simulation utilized in the following sections.
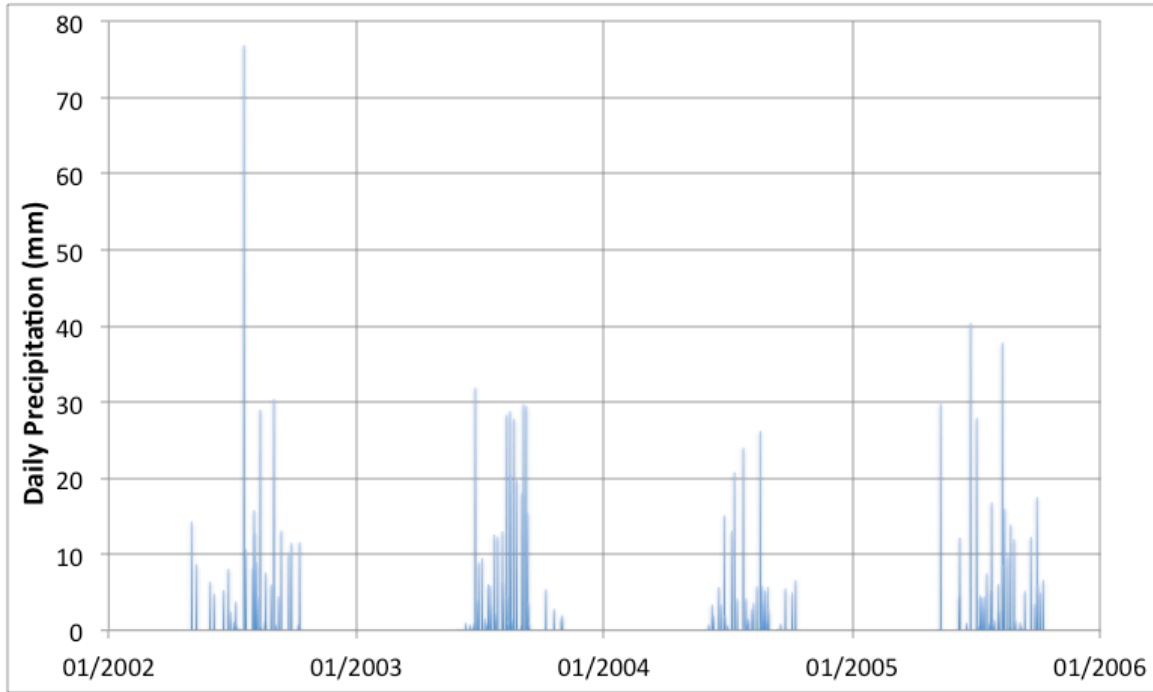
*Figure 4.1*: Daily Precipitation measured at the AMMA site near Agoufou

To test model performance, in lieu of streamflow or stage data as discussed previously (*Section 3.7*), 10 LANDSAT images of lake area between 2002-2006 were converted to lake volume using *equation 3.8* [*Table 4.1*]. These 10 data points were compared to predicted lake volumes from SWAT using two different statistical measures of model performance: the coefficient of determination ($R^2$) and the Nash-Sutcliffe model efficiency coefficient (NSE). Attempting to measure model efficiency with only 2 metrics and with only 10 data points is an imperfect solution; nevertheless, a metric was necessary to compare each run of the model. The main objectives of these simulations were to (1) provide a preliminary calibration for SWAT in Agoufou basin, and (2) provide a starting point for calibration and verification of post-drought model parameters for long-term simulation.

*Table 4.1*: LANDSAT Lake Areas and estimated lake volumes

| Image Date | LANDSAT Lake Area (m²) | Estimated Lake Volume (m³) |
|---|---|---|
| 3/11/02 | 1641735 | 894975 |
| 5/30/02 | 1065465 | 564000 |
| 6/1/02 | 1086677 | 576000 |
| 9/3/02 | 5764010 | 3422325 |
| 10/24/03 | 6002712 | 3573900 |
| 7/6/04 | 1345844 | 723825 |
| 9/24/04 | 2386092 | 1334250 |
| 11/11/04 | 1687809 | 921825 |
| 4/4/05 | 674793 | 346275 |
| 10/30/05 | 2667446 | 1502925 |

Manual "trial and error" calibration of the most sensitive model parameters [*Table 3.*4] coupled with knowledge of basin characteristics and sensitivity analysis of model parameters was performed for the four years of available precipitation data. Ranges of acceptable parameter values based on physical basin characteristics were not exceeded [*Tables 3.2 & 3.3*]. Automatic calibration procedures would be practically useless for Agoufou, as they typically require concurrent streamflow or stage data to compare with simulated data for best results. Given that only four years of precipitation forcings were available and that these simulations were only a preliminary test of model functionality and performance, no verification was performed. The best-fit to lake volumes [*Table 4.2*] in terms of $R^2$ (0.936) and NSE (0.921) is shown in *Figure 4.2*.  The performance of the model is impressive, capturing a large fraction of the variability in lake volume changes during the four-year period.

*Table 4.2*: SWAT model parameters for "best-fit" scenario of short-term simulation

| Parameter Name: | Parameter Description: | Best-fit Value:<br>[Green / Red/ Blue / Yellow] |
|---|---|---|
| CN2 | Curve Number for Moisture Condition #2 | [50 / 39 / 85 / 74] |
| ESCO | Soil Evaporation Compensation Factor | 0.75 |
| SOL_Z | Depth of Soil ($m$) | [3.0 / 1.5 / 0.3 / 0.01] |
| SOL_K | Hydraulic Conductivity of Soil ($mm\ hr^{-1}$) | [300 / 120 / 50 / 5] |
| SOL_ALB | Wet soil albedo | [0.20 / 0.22 / 0.16 / 0.1] |
| SOL_AWC | Plant available water capacity ($mm\ H_2O\ mm^{-1}\ soil$) | [0.13 / 0.18 / 0.1 / 0.01] |
| RES_K | Infiltrability of Lake Bottom ($mm\ hr^{-1}$) | 0.4 |
| RCHRGDP | Aquifer Percolation Coefficient | 0.45 |
| GWQMN | Threshold water level in aquifer for baseflow ($mm$) | 5 |
| OV_N | Manning's n for Overland Flow | [0.15 / 0.20 / 0.15 / 0.1] |
| BLAI | Maximum Leaf Area Index ($m^2\ m^{-2}$) | [1.5 / 2 / 1.5 / 0.3] |
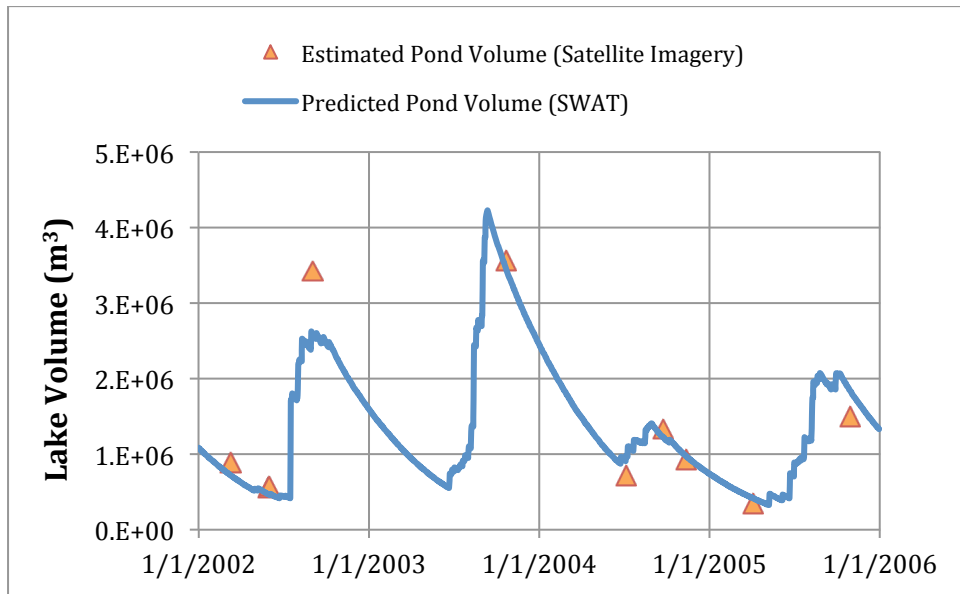


*Figure 4.2*: "Best-fit" scenario of simulated lake volume over time

40

Results from the best-fit scenario are shown in *Figures 4.3-4.6. Figure 4.3* contains surface and subsurface runoff partitioning for 2003 over the entire basin. Over the full four-year period, surface runoff contributes 82% of the total runoff, while subsurface flow contributes the final 18%. To address project hypotheses, the partitioning of surface and groundwater runoff is extremely important. We know that during pre-drought conditions surface runoff was suppressed by the presence of woody vegetation and stable soils where hardpan and shallow soils now exist. While it is likely that surface flow was still the dominant runoff mechanism under pre-drought conditions, the disparities between surface and subsurface partitioning and runoff volumes were likely reduced. Prior to soil and vegetation degradation, much smaller surface runoff volumes should be expected. *Figures 4.4-4.6* show the spatial variability of simulated surface and subsurface flow as well as the soil moisture content at the subbasin level following a 75 mm storm on July 18th, 2002. As expected, the majority of the simulated surface runoff originates from the northern portion of the basin where hardpan and shallow soils prevail, and the majority of the simulated subsurface flow originates from the southern and western portions of the basin where deep sands and greater slopes dominate. Precipitation does not infiltrate as quickly as in the northern basin due to the prevalence of hardpan, and the subsurface flow that is simulated is due to return flow from the deeper sand lenses. An insignificant amount of deep aquifer percolation occurs since most of the water either stagnates and evaporates or runs off into a system of rills and eventually into the stream network. Minimal vegetation exists to provide the capillary pressure to hold water in the sand lenses, so most of the water that infiltrates is released quickly and contributes to streamflow and thus lake volume.
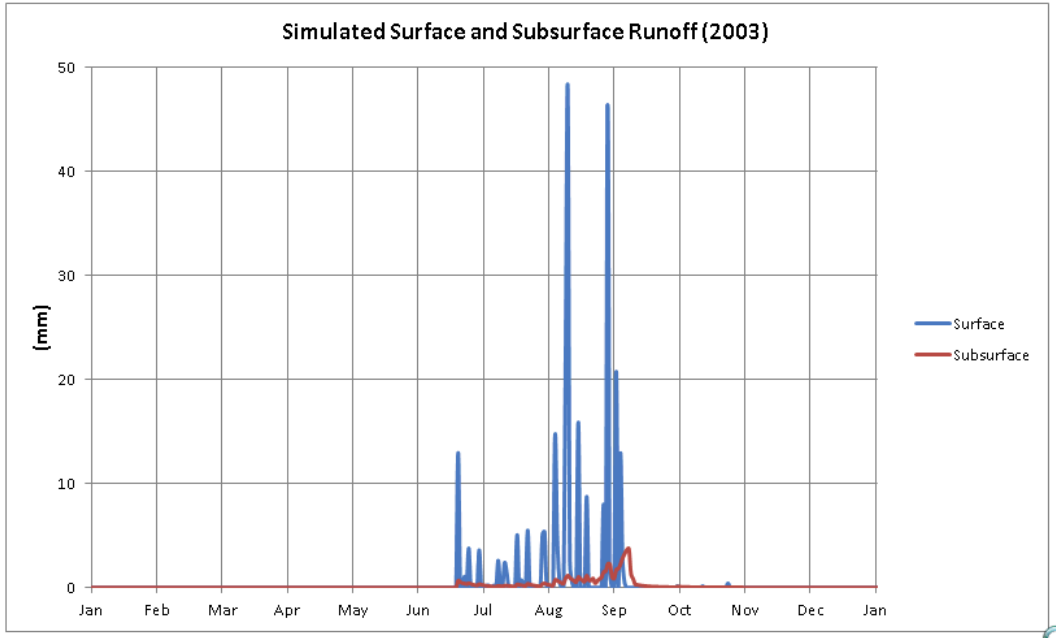
*Figure 4.3*: Simulated Surface and Subsurface Runoff for 2003
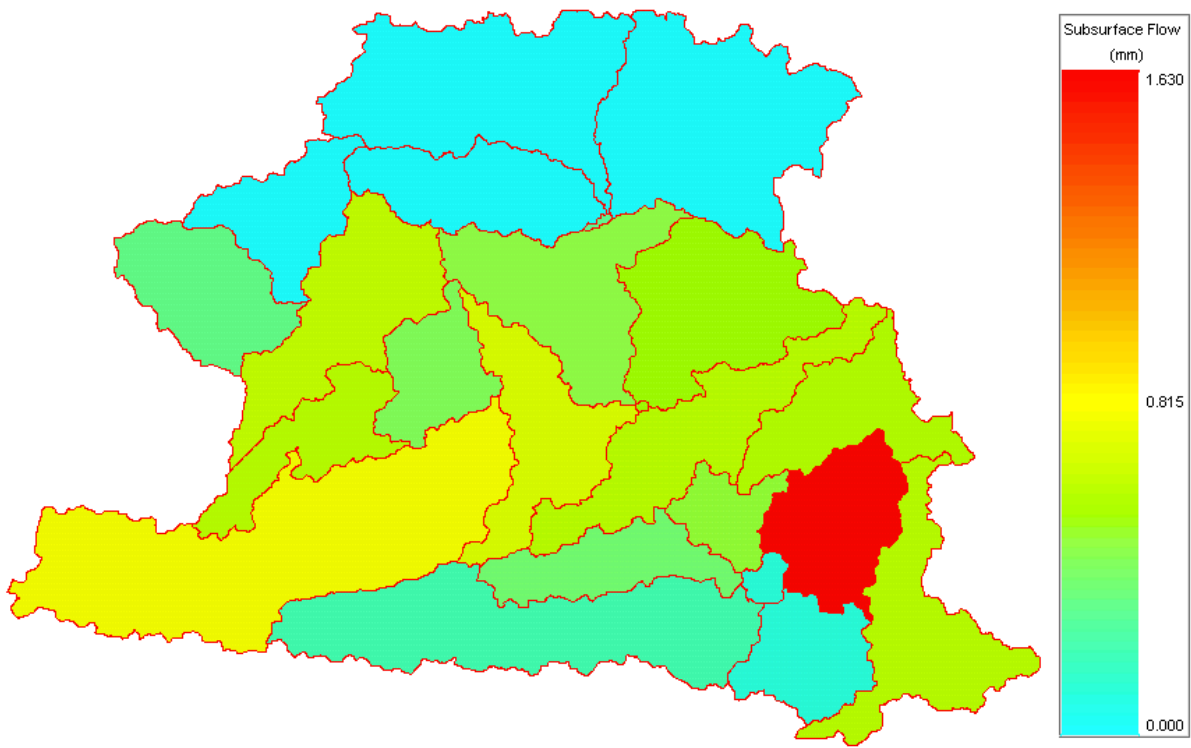


*Figure 4.4*: Spatial variability of simulated subsurface flow following a 75 mm rainstorm on July 18th, 2002
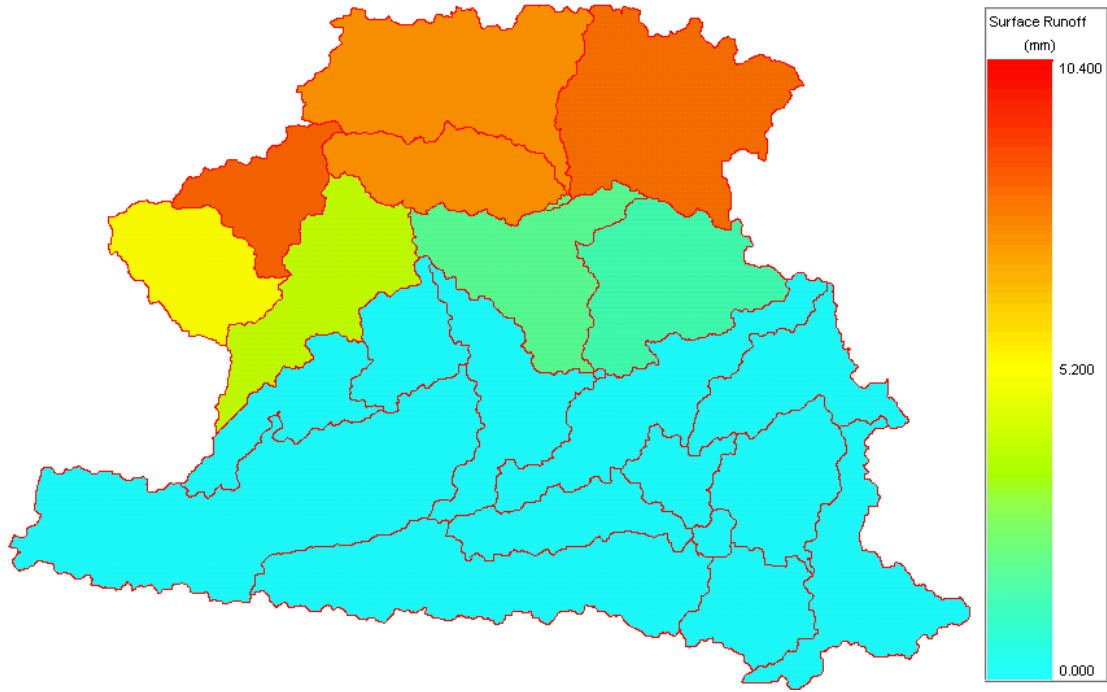
*Figure 4.5*: Spatial variability of simulated surface flow following a 75 mm rainstorm on July 18th, 2002
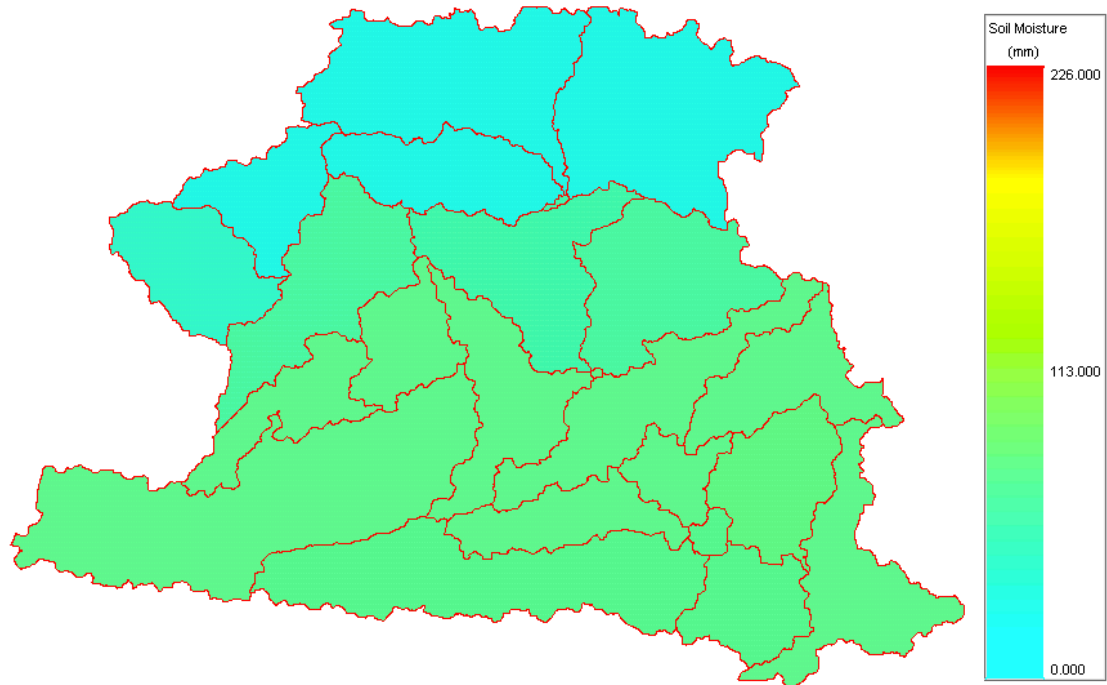


*Figure 4.6*: Spatial variability of simulated soil moisture following a 75 mm rainstorm on July 18th, 2002

*Figures 4.4-4.6* provide a picture of the spatial variability of basin response due to a large convective storm system. Antecedent conditions were quite dry, with only a few mild and sporadic storms previously, as can be seen in *Figure 4.1*. The varied response of different soils is blatantly clear in the figures. The main drivers of variability are soil type, soil depth, and vegetation. In the North there is very little soil moisture and almost no subsurface flow. The south sees a large increase in soil moisture and thus responds with subsurface flow, albeit with much less volume than from the surface flow in the North. The transition zone between high runoff and low runoff areas of the basin is also evident in the output. These outputs suggest that the model is able to predict the anticipated spatial response patterns, despite the unorthodox data-gathering techniques employed for parameterization.

The important takeaway from the preliminary calibration is whether or not SWAT can adequately predict hydrologic response in this data-scarce region. In addition, can the model, once coupled, provide acceptable results to test the overall project hypotheses from *Section 2.2*? The project hypotheses will require the coupled models (*see Section 2.2*) to simulate spatial variability of hydrologic response due to changes in vegetation, soils, and human development. Given the spatial variability of response shown and degree of accuracy of lake volume prediction, it is clear that SWAT has the capability to provide a suitable tool for testing these hypotheses.

*4.2: Long-term simulation of post-drought Agoufou*

While calibrating SWAT with four years of data produced satisfying results, to properly test project hypotheses, long-term simulation of the basin is required. To simulate

longer periods of time, downscaled synthetic precipitation (*Section 3.5*) from the coarse regional datasets, CRU and TRMM, is used. It is not expected that simulated basin response in the form of lake volumes "fit" the observed LANDSAT imagery nearly as well as simulated basin response forced by daily data measured three kilometers from the basin. Although greater storage volume differences will most certainly arise, the important takeaways from long-term simulations are emergent patterns in vegetation and runoff due to changes in climate and human activities in the region. What are the dominant processes that have caused a lake-state change from ephemeral to perennial in this basin? Are human activities in the region maintaining the vegetation degradation that occurred after the Great Sahelian Drought (GSD)? Could humans be increasing the level of degradation or is their effect on the basin minimal? Could the basin have responded to a return in average rainfall by returning to an ephemeral state had no human intervention occurred? These and other related questions can only be addressed with long-term simulation of the basin.

The first series of long-term simulations were run over the years following the Great Sahelian Drought (1985-2011). During this time, it is known that a massive die-off of woody vegetation occurred (*see Sections 1 & 2*). Following the die-off, soil once held in place by woody vegetation has slowly eroded to its current degraded state. SWAT cannot dynamically change model parameters, and thus does not automatically change soil and vegetation parameters given a changing climate. However, the model parameters must change based on changes in vegetation, soil, and land cover witnessed during this period. To demonstrate this basin change, it is assumed that the functions of all temporal parameter changes relating to affected basin behavior following the Great Sahelian Drought are linear.

Assuming linear parameter change implies that the soil and the vegetation in the northern portion of the basin have been slowly degrading at a constant rate over time for the last 27 years. Without vegetation, the shallow sand lenses covering the hardpan in the North are continuing to erode over time, expanding the amount of area that is covered by hardpan. SWAT does not have the capability to dynamically re-map the basin area into new HRUs, i.e. new land cover and soil classes, over time. The vegetation map used to describe the land cover and soil classes was developed in 2012; therefore it does not describe the physical state of the watershed in 1985. The parameters of the northern portion of the basin that are used for simulating basin response in 1985 will be a best-guess average of what the physical state of the basin was at the time. The information we do possess for that time is that the lake was ephemeral, woody vegetation thrived in the North, and human interaction with the basin was only seasonal. Over the past 27 years, the respective areas and physical properties of the hardpan and sand lenses have changed, so our goal is to attempt to average the combination of responses of the two classes to most closely resemble the physical response of the watershed as it has degraded over time.

This dynamic change was coded into SWAT, overriding model parameters each year. For example, pre-drought levels of the Curve Number (CN2) model parameter values for affected basin areas are assumed to increase linearly to present day levels:

$$(Eq. 4.1) \quad CN2_t = CN2_0 + t\left(\frac{CN2_{27} - CN2_0}{27}\right)\Bigg|_{t=0-27}$$

where $t$ is the year beginning in 1985 and ending in 2011, $CN2_{27}$ and $CN2_0$ are present day and 1985 levels of the Curve Number model parameter, respectively. The affected basin areas include the northern portions of the basin where woody vegetation bands once

existed. The grassy rangelands covering dunes in the south have mostly recovered and were therefore not expected to see much of a change in model parameters. *Table 4.3* details the changes in model parameters from 1985-2011.

*Table 4.3*: SWAT parameters affected by dynamic linear change

| Parameter Name: | Parameter Description: | Best-fit Value for 1985: [Green / Red/ Blue / Yellow] | Best-fit Value for 2011: [Green / Red/ Blue / Yellow] |
|---|---|---|---|
| CN2 | Curve Number for Moisture Condition #2 | [45 / 35 / 65 / 65] | [55 / 42 / 90 / 85] |
| BLAI | Maximum Leaf Area Index $(m^2\ m^{-2})$ | [1.5 / 2 / 1.5 / 1.5] | [1.5 / 2 / 1.5 / 0.3] |
| SOL_Z | Depth of Soil $(m)$ | [3.0 / 1.5 / 1.0 / 0.5] | [3.0 / 1.5 / 0.2 / 0.01] |
| SOL_K | Hydraulic Conductivity of Soil $(mm\ hr^{-1})$ | [300 / 120 / 100 / 75] | [250 / 125 / 50 / 5] |
| SOL_AWC | Plant available water capacity $(mm\ H20\ mm^{-1}\ soil)$ | [0.15 / 0.20 / 0.15 / 0.1] | [0.15 / 0.20 / 0.15 / 0.01] |

As in the previous section, the model was calibrated using a "trial and error" procedure. The first 10 years (1995-2005) served as the calibration period, and the model was then run and verified over the total 27-year period. This 10-year period was chosen due to its rapid increase in lake volume, in addition to the fact that it also covered both wet and dry years. At the beginning of this period, it was becoming clear that the perennial state of the lake would become permanent. By the end of the period, permanent human settlements had been established near the Lake for some time and the perennial state of the lake seemed to have become irreversible. The 10-year range of parameters for the linear change was adjusted hundreds of times, and the static parameters were adjusted slightly as well. As before, the physical range of accepted parameters was not exceeded. Once an acceptable parameter set was found, the linear changes were extrapolated to the

entire 27-year period. The objectives of this series of simulations were to (1) verify model parameters used in Section 4.1, (2) modify parameters if necessary, (3) test the validity of assuming linear temporal parameter change, and finally (4) validate the model for this 27-year period. Thirty-nine LANDSAT images of lake extent exist for this period of simulation.

The "best-fit" results of the calibration procedure in terms of simulated lake volumes over time are shown in *Figure 4.7*. Visually, the model simulates lake volume quite well except for three obvious outliers: two data points in the wet season of 1999 and one in the wet season of 2002. The remaining data points are predicted with great accuracy. Any effort to adjust the model parameters such that the simulated lake volume in 1999 was reduced to a more reasonable level resulted in large discrepancies for the remaining years of the simulation. Given the regional downscaled climate forcings driving the simulation, no physically acceptable parameter set will allow the model to perfectly align the simulated lake volumes with the available LANDSAT-derived lake volume data points. Ultimately, it is more important for the physical properties of the watershed to be properly reflected with model parameters than to perfectly simulate lake volumes. Quantifiable results of the 10-year calibration and subsequent validation in terms of NSE and $R^2$ are shown in *Table 4.4*.
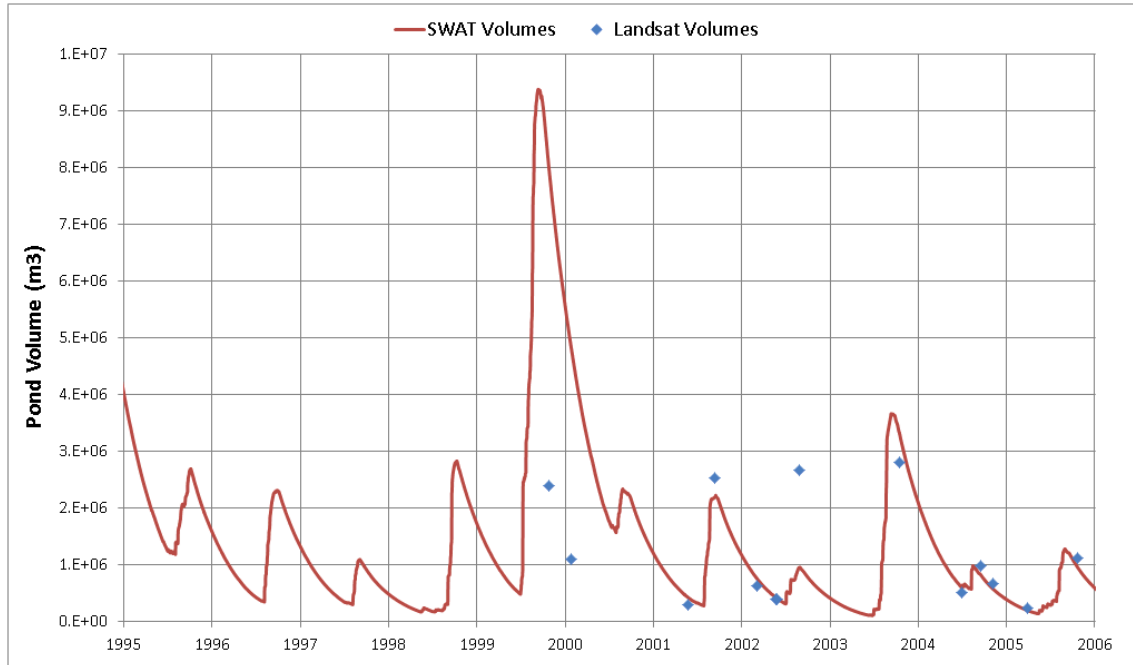
*Figure 4.7*: Lake volume time series for the calibration of SWAT from 1995-2005.

*Table 4.4*: Results from Calibration and Validation of SWAT for 1985-2011

|  | Calibration | Validation |
|---|---|---|
|  | *1995-2005* | *1985-2011* |
| $R^2$ | 0.334 | 0.417 |
| NSE | -2.987 | -0.615 |

It is readily apparent that the numerical results are quite poor. The error is largely due to high annual rainfall total (520 mm) in 1999, approximately 150 mm above MAP for Agoufou. In addition, 400 mm of this rainfall—which would also be above MAP for Agoufou—fell in just two months: July and August. The downscaling procedure utilized in *Section 3.5* cannot completely account for the extremes of monthly precipitation. The total precipitation simulated for these two months occurs in 5-10 events, depending on the

subbasin. With such high intensity rainfalls—up to 125 mm for one day in some areas—it is understandable that a surface runoff-dominated watershed would see a huge increase in lake volume as a result. In reality, given the amount of precipitation in July and August, it is likely that the rain would have been spread out over many more than 5-10 events, decreasing the intensity of each storm such that less water escapes infiltration and ends up in the lake. Instead of introducing subjective bias by manually adjusting the precipitation forcings, the above result was accepted. This decision was made after repeated re-simulation of the precipitation forcings using the procedure in *Section 3.5* with little change in model behavior.

However, to ensure that the model was performing well despite a poor 1999, the two outliers were neglected and the numerical model efficiency metrics were recalculated. Significantly better results are shown in *Table 4.5*. The entire 27-year period of simulated lake volumes from model verification is shown in *Figure 4.8*. Visually, the model simulates lake volumes well other than in 1999 and 2002. The model under-predicts lake volume in 2002 and 2011, and over-predicts lake volume in 2007. It is expected that the model does not perform nearly as well when driven by regional climate data as opposed to local gage data. Regional datasets cannot perfectly capture the variability of an entire region, especially for a climatically extreme region such as the Sahel.

Table 4.5: Results from Calibration and Validation of SWAT for 1985-2011; neglecting outliers in 1999.

| | Calibration | Validation |
|---|---|---|
| | *1995-2005* | *1985-2011* |
| $R^2$ | 0.703 | 0.563 |
| NSE | 0.681 | 0.32 |
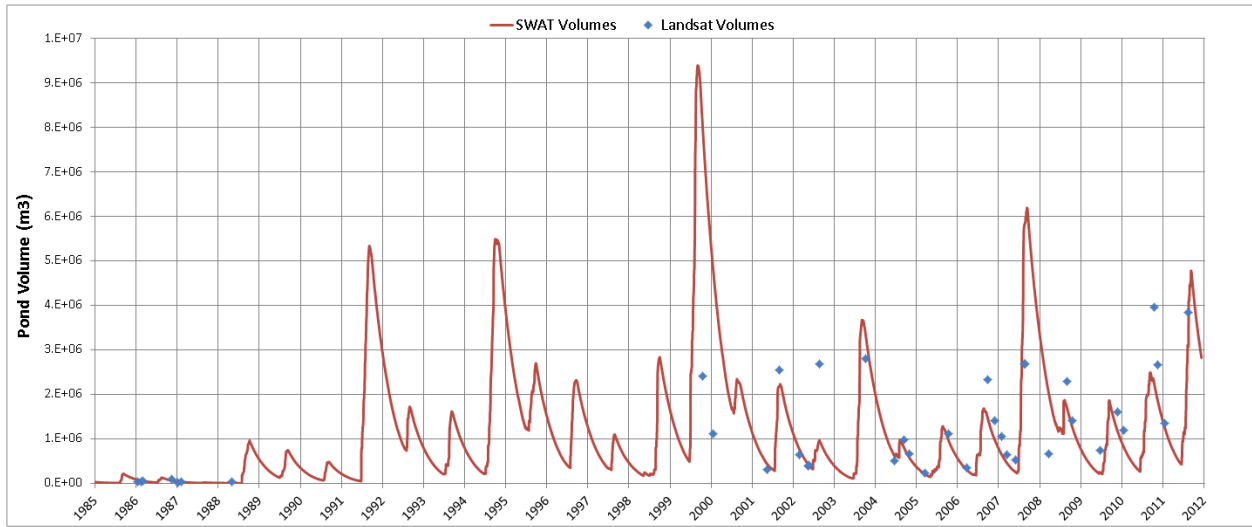


Figure 4.8: Lake volume time series for the validation of SWAT for 1985-2011

The model predicts the lake-state change from ephemeral to perennial at approximately the correct time (~1989), preliminarily suggesting that assuming linearity for temporal parameter change over this period may be an adequate depiction for temporal basin dynamics. Except for wet and dry years, the average lake volume at the end of the dry season—the lowest water level of each year—continues to steadily increase throughout the simulation, which is consistent with the available LANDSAT imagery and anecdotal data.

The SWAT "best-fit" parameters for long-term simulation of post-drought Agoufou are compared with those from *Section 4.1* in *Table 4.6*. Since some of the parameters are

changing over time (*Table 4.3*), those depicted in *Table 4.6* were chosen from the end of

2004. This year coincides with the middle of the four-year simulation shown in *Section 4.1*.

The necessary modifications in parameters are due mostly to changing soil and vegetation

properties in the northern portion of the basin. However, the parameter for reservoir

bottom infiltration (*RES_K*) changed as well to slightly modify the timing and volume of the

peaks and valleys of the lake volume hydrograph. Most of the other sensitive parameters

were only changed slightly, and many were not changed at all.

Table 4.6: SWAT "best-fit" parameters for long-term simulation of post-drought Agoufou,
compared with those from *Table 4.2* of *Section 4.1*.

| Parameter Name: | Best-fit Value (short-term): [Green / Red/ Blue / Yellow] | Best-fit Value (long-term): [Green / Red/ Blue / Yellow] | Percent Difference (%): |
|---|---|---|---|
| CN2 | [50 / 39 / 85 / 74] | [53 / 40 / 84 / 80] | [+6 / +3 / -1 / +8] |
| ESCO | 0.75 | 0.94 | +25 |
| SOL_Z | [3.0 / 1.5 / 0.3 / 0.01] | [3.0 / 1.5 / 0.4 / 0.1] | [0 / 0 / +33 / +900] |
| SOL_K | [300 / 120 / 50 / 5] | [262 / 124 / 62 / 21] | [-12.7 / +3.3 / +62 / +320] |
| SOL_ALB | [0.20 / 0.22 / 0.16 / 0.1] | [0.20 / 0.22 / 0.16 / 0.1] | 0 |
| SOL_AWC | [0.13 / 0.18 / 0.1 / 0.01] | [0.13 / 0.18 / 0.1 / 0.03] | [0 / 0 / 0 / +200] |
| RES_K | 0.4 | 0.7 | +75 |
| RCHRGDP | 0.45 | 0.42 | -7 |
| GWQMN | 5 | 6.5 | +30 |
| OV_N | [0.15 / 0.20 / 0.15 / 0.1] | [0.15 / 0.20 / 0.15 / 0.1] | 0 |
| BLAI | [1.5 / 2 / 1.5 / 0.3] | [1.5 / 2 / 1.5 / 0.6] | [0 / 0 / 0 / +100] |

*Figures 4.9 & 4.10* show surface and subsurface runoff partitioning over the entire

basin for 1991 and 2009. In 1991, subsurface flow accounts for 59% of total runoff, while

surface flow contributes the remaining 41%. In 2009, these numbers drastically switch to

30% and 70%, respectively. Over the entire 27-year period, surface runoff contributes 53% of the total runoff, while subsurface flow contributes the final 47%. Surface runoff does not dominate total runoff volume in the region immediately post-drought as was originally expected. We overestimated of the speed of system-level response to the eco-hydrologic effects of the drought. It seems that although much of the woody vegetation in the North had perished immediately following the drought, one reason that it is possible to see a delayed erosion response is that the roots may have still been holding soils into place for years after the drought.
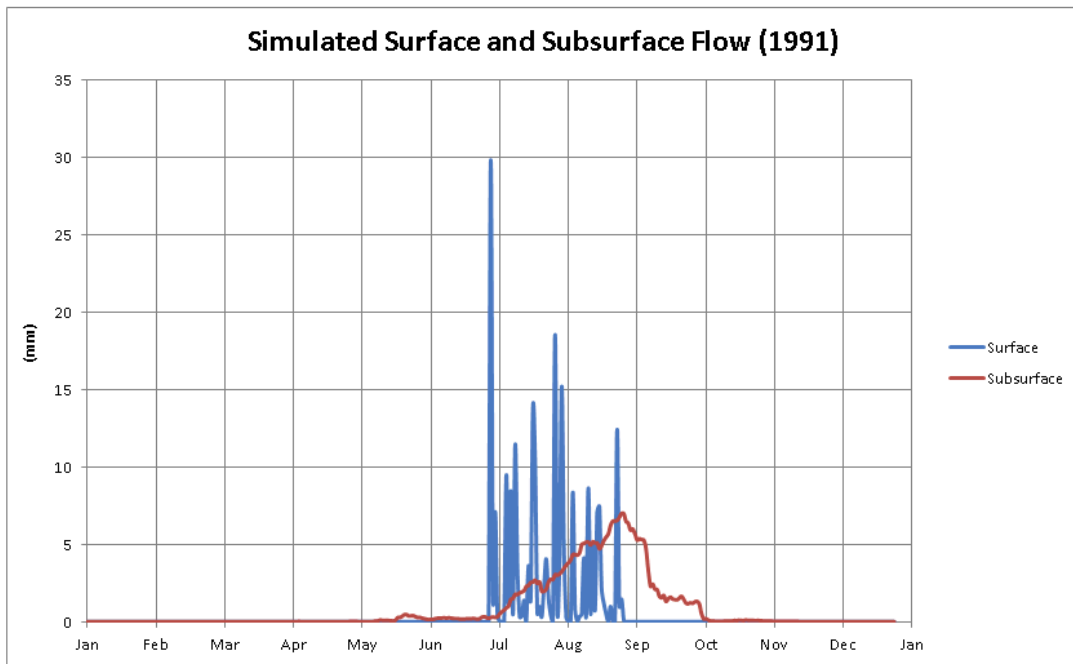


*Figure 4.9*: Simulated Surface and Subsurface Runoff for 1991
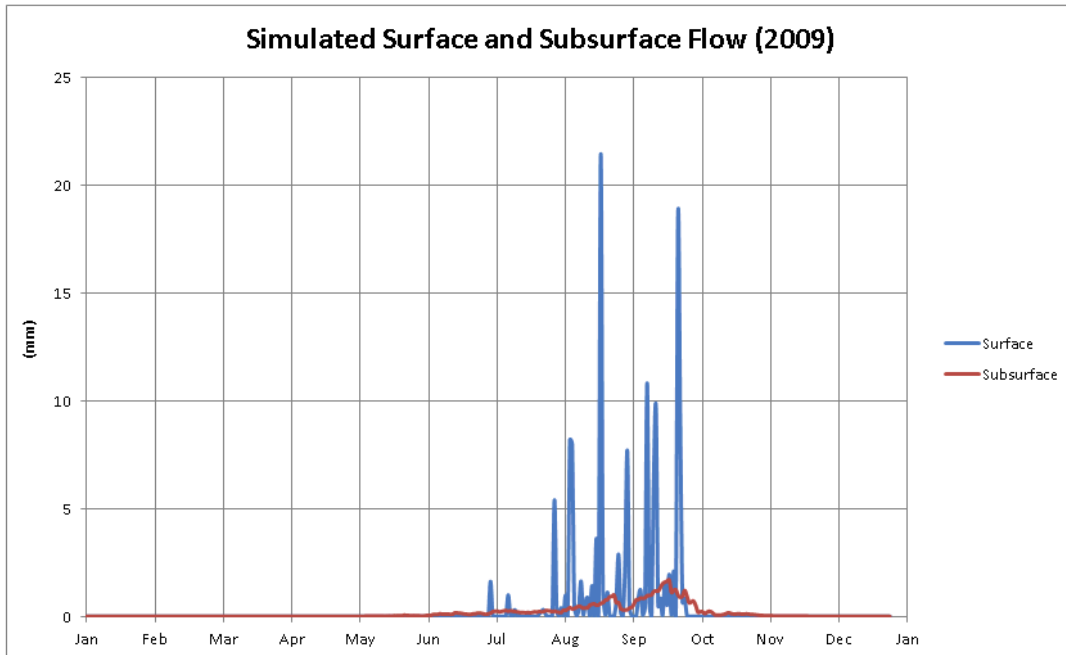
*Figure 4.10*: Simulated Surface and Subsurface Runoff for 2009

To visualize the spatial heterogeneity of basin response for the long-term simulations in this section (*4.2*) as was done in the previous section (*4.1: Figures 4.4-4.6*), it was necessary to sum the responses of each subbasin for each month. Since precipitation does not fall uniformly over the entire watershed, as was the case previously, it is difficult to capture spatial variability of different runoff mechanisms in the same figure without summing responses over each month. Total monthly precipitation for each subbasin is equal; therefore, comparing their monthly responses will allow us to assess how the watershed is behaving spatially. There can, however, be differences in response due to the timing and intensity of the simulated storms, so while we will use this method to plot results from the simulation, the reader should understand that response is subject to intensity of storms as well as antecedent conditions.

54

*Figures 4.11-4.13* show the spatial variability of simulated surface and subsurface flow as well as the level of soil moisture summed monthly at the subbasin level for August 1991. The figures are meant to show conditions of the basin upon the return of average rains following the Great Sahelian Drought, where vegetation death has occurred but degradation of the soils has just begun. The majority of the simulated subsurface flow still originates from the southern portion of the basin, but a slight response from the northern basin is present where it was not seen in the previous section. Not much change from the figures in *Section 4.1* can be seen here, but that is because the southern portion of the basin consists largely of dunes covered in annual grasses that recovered quickly upon the return of the rains to the region following the GSD. Subsurface flow levels are only slightly higher, predominantly driven by the central areas of the basin, where sand lens depths have not yet degraded to present-day levels and thus are contributing more to subsurface flow volumes rather than surface flow volumes. Surface runoff still predominantly originates from the Northern portion of the basin, especially in areas were hardpan exists. However, the level of surface runoff is greatly diminished. In *Figure 4.5* the surface runoff response is approximately half that of *Figure 4.12*, but it is responding to a large storm on a single day. *Figure 4.12* shows the total surface runoff for the entire month of August. Similarly to the levels of subsurface flow, the level of soil moisture in *Figure 4.13* is larger than that of *Figure 4.6*, due to the presence of a larger soil column for storage in sand lenses.
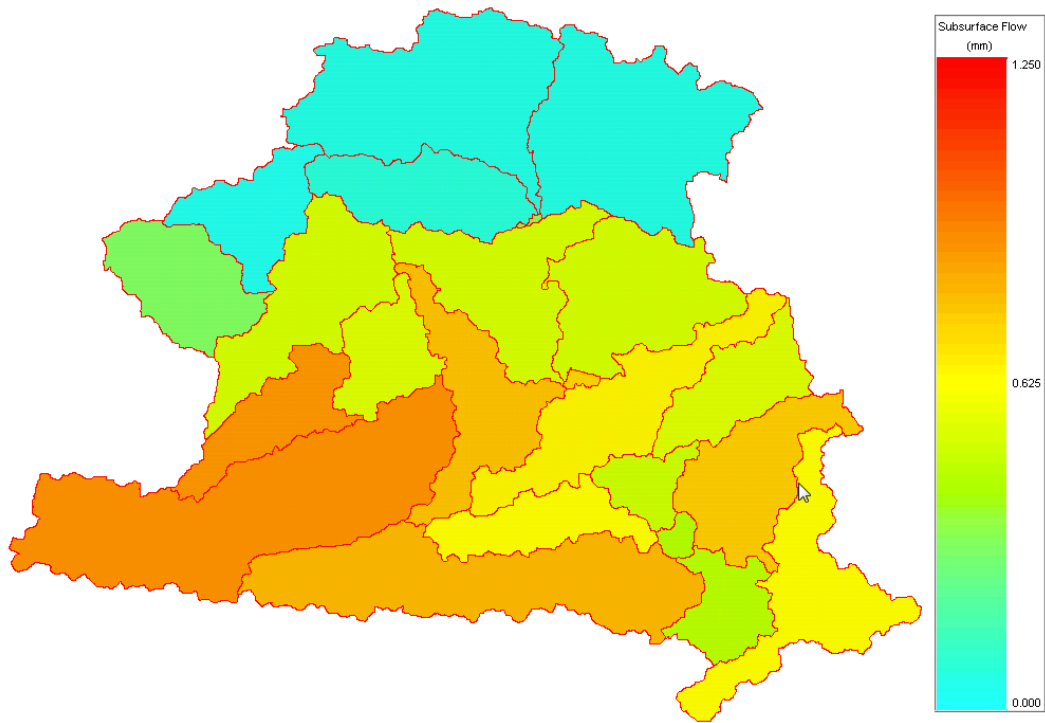
*Figure 4.11*: Spatial variability of simulated subsurface flow for the month of August in 1991.
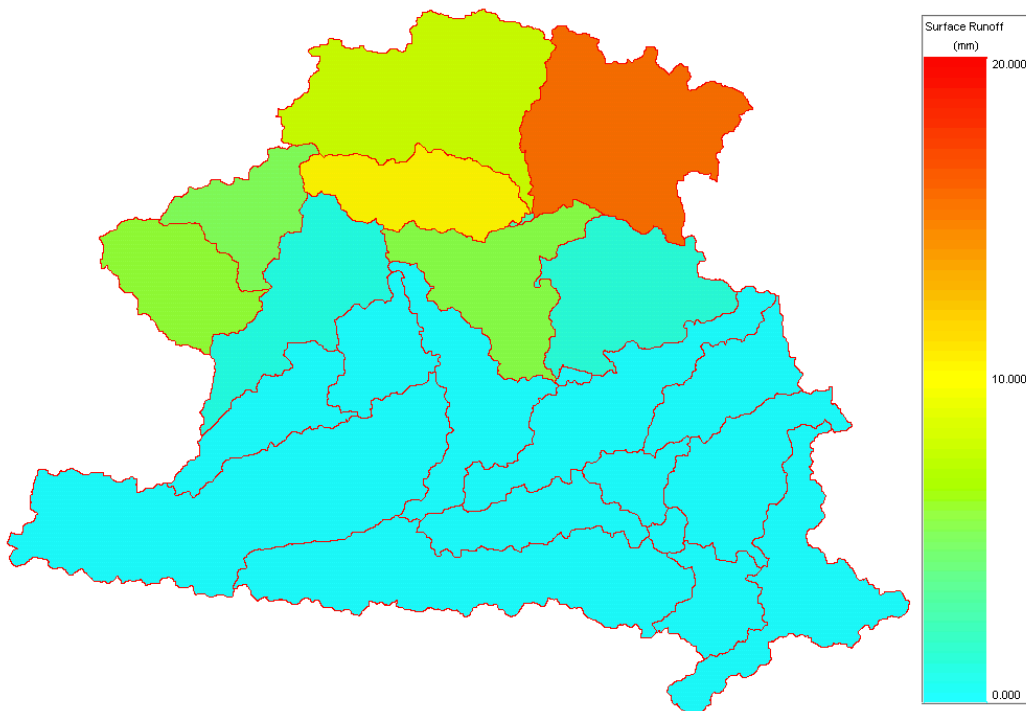


*Figure 4.12*: Spatial variability of simulated surface runoff for the month of August in 1991.

*Figure 4.13*: Spatial variability of simulated soil moisture for the month of August in 1991.
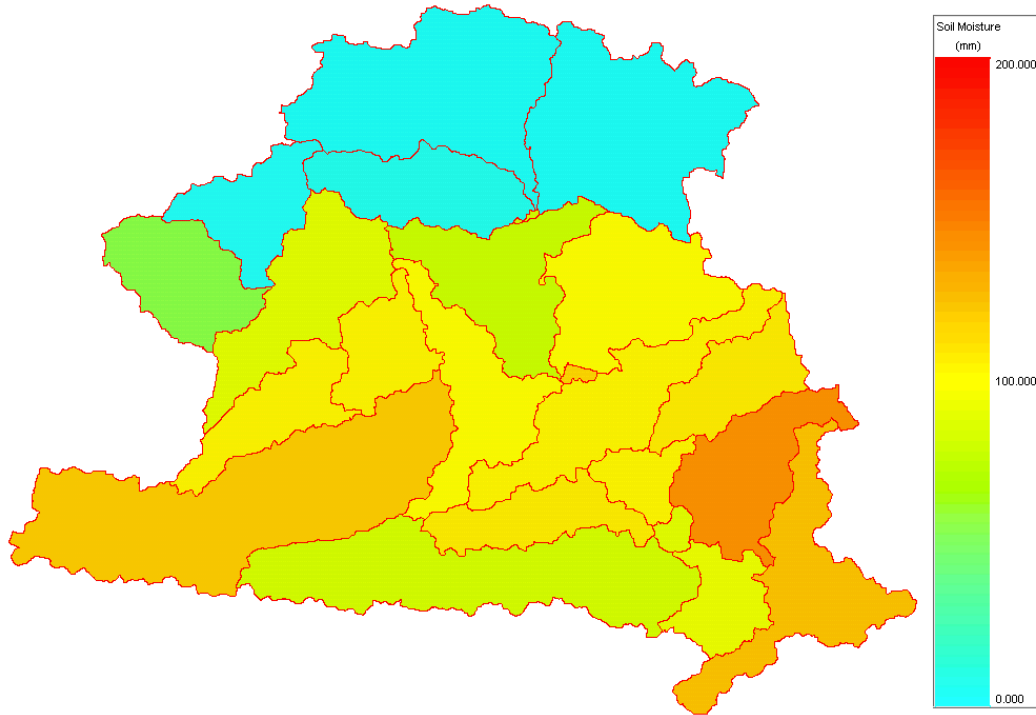
*Figures 4.14-4.16* show the spatial variability of simulated surface and subsurface flow as well as the level of soil moisture summed monthly at the subbasin level for August 2009. The figures are meant to show conditions of the basin at close to present-day conditions, where vegetation death is a thing of the distance past and degradation of soils has already occurred and may be still occurring in the North. The majority of the simulated subsurface flow still originates from the southern portion of the basin, and northern basin subsurface response is negligible. Subsurface flow levels are slightly lower, with less subsurface flow coming from sand lenses on hard pan however this could be due to less precipitation. Surface runoff predominantly originates from the Northern portion of the basin, and the volume is much larger due to increased degradation of soils in the area. Soil

moisture is much the same as it has been in the past simulations, indicating no basin change.
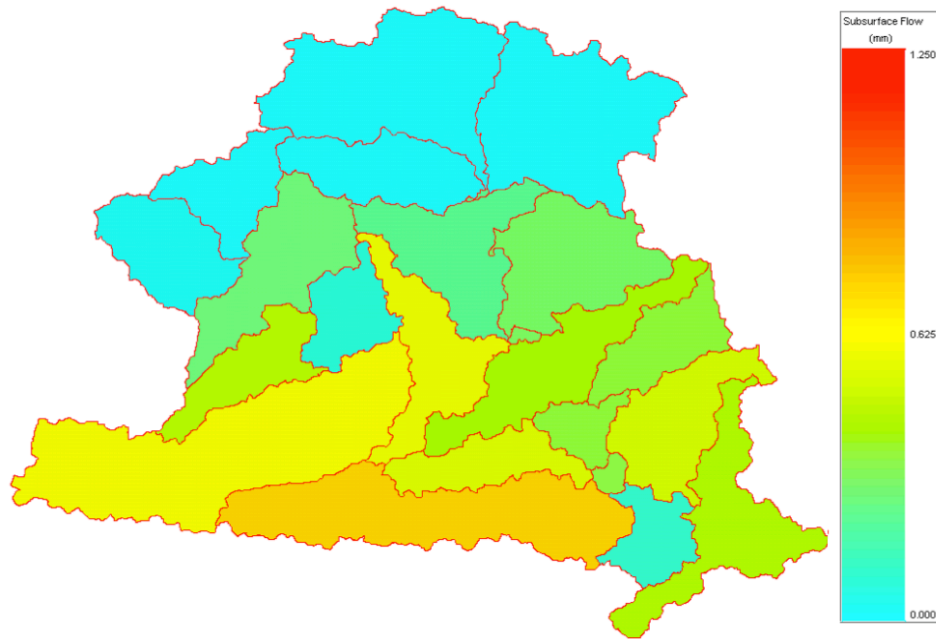


*Figure 4.14*: Spatial variability of simulated subsurface flow for the month of August in 2009.
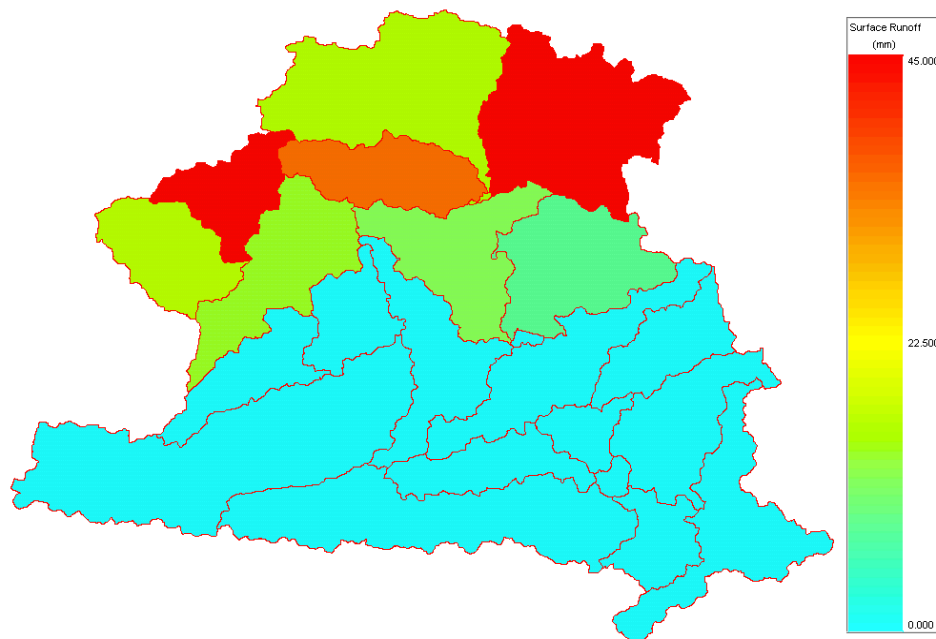


*Figure 4.15*: Spatial variability of simulated surface runoff for the month of August in 2009.
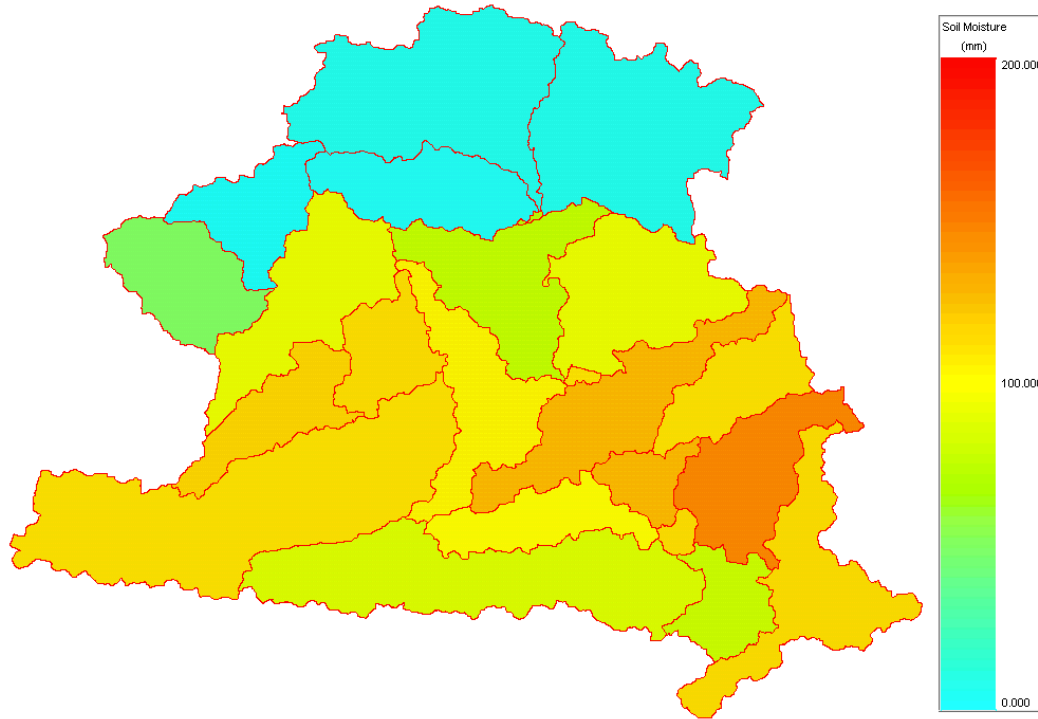
*Figure 4.16*: Spatial variability of simulated soil moisture for the month of August in 2009.

The assumption of linearity in regards to the temporal changes in soil and vegetation parameters in the northern portion of the basin is put to the test in this section. The model simulated an emergent lake-state change from ephemeral to perennial at approximately the correct point in time, directly due to the increased runoff from the northern portion of the basin. Parameter stationarity over the entire period would not have produced the same results. However, other options to simulate similar response exist and could have been chosen. For example, it could be assumed that all or most of the soil once held in place by woody vegetation was eroded in the few years shortly after the GSD. The case against this hypothesis is that the level of the lake has continued to rise into the new millennium without a corresponding increase in precipitation. If the current state of the basin has not changed in 20 years, then there should be no continued increase in lake

volume. It could also be argued that increased surface runoff is only part of the picture. Increased runon infiltration and subsequent return flow could also have an effect on increased lake volumes. Or, it could be that the lake is hydrologically connected to a shallow aquifer. While both are interesting ideas, it is known that Agoufou Lake sits atop an exposed section of the impervious continental terminal, hydrologically disconnected from the aquifer. It is safe to assume that the physical characteristics of the watershed have been changing temporally since the end of the GSD, and that they have continued to change at least into the first decade of the new millennium. While the temporal changes in basin parameters may not have been linear, the assumption of linearity is convenient and could average out nonlinear fluctuations in those changes. For example, given the rapid increase in lake volume over the past two decades, it could be assumed that the change is exponential, occurring much more rapidly than linear. However, there is only so much soil to erode away, and while erosion is the norm, many of the sand lenses covering hard pan are growing due to wind redistribution behind topographic features. The point is, while the increases may have been rapid, eventually they will slow down. The curve numbers used in this simulation near the end of the 27-year period are approaching that of urban, paved areas. They cannot get much higher than they already are. So if the changes were indeed exponential at first, they would begin or have already begun to decay.

The long-term simulations shown in this section prove that interesting results from hydrologic modeling exercises can be obtained even in data-scarce regions of the world. Typically, hydrologic model calibration with concurrent streamflow data can yield values of approximately 0.75-0.85 for both $R^2$ and NSE. While calibration and validation of SWAT produced model efficiency values [*Tables 4.4 & 4.5*] that might seem unacceptable for

hydrologic simulation of a data-rich region, given the scarcity of available data for parameterization and calibration as well as the assumptions involved in forcing the model (detailed in the previous sections), the author argues that the result is more than acceptable. The situation is difficult, of course, but that is why it is necessary to resort to unorthodox techniques to glean whatever is possible from model behavior while keeping in mind the assumptions made to achieve the result.

*4.3: Full length simulations of pre- and post-drought Agoufou*

Armed with knowledge of basin parameters from the previous two sections, it is now possible to simulate basin response for both pre- and post-drought Agoufou, from 1901-2011. Unfortunately LANDSAT imagery of pre-drought Agoufou does not exist, so no lake extent measurements will be used to validate the model prior to 1986. While data was scarce post-drought, it is almost nonexistent pre-drought. There is little that can be added to the analysis of *Sections 4.1 & 4.2*. However, it is known that the lake was fairly drastically ephemeral except in abnormally wet years. We do not know whether or not the basin remained ephemeral every year because records do not exist, but we do know that it was drastic enough such that only seasonal grazing was commonplace, therefore a perennial lake-state should be considered an uncommon occurrence prior to the 1990s.

*Figure 4.17* contains the full-length, 111-year simulation of lake volumes at Agoufou. From 1985-2011, the parameters are exactly the same as what is shown in *Table 4.6* of *Section 4.2*. From 1901-1984, basin parameters were assumed to be stationary. Since 1985 marked the end of the GSD, the parameters used for 1901-1984 indicate slightly less-degraded soils from those shown in *Table 4.3*—i.e. slightly lower curve numbers, slightly

61

higher soil depths, and slightly higher hydraulic conductivities—but are more or less the same. Changes were less than five percent in all cases. Without slight adjustment, there were often multiple year periods of perennial lake-states simulated throughout the period. While there is knowledge of droughts and wet periods throughout the past century, no permanent lake-state change occurred and the basin remained only a seasonal destination for transhumants.
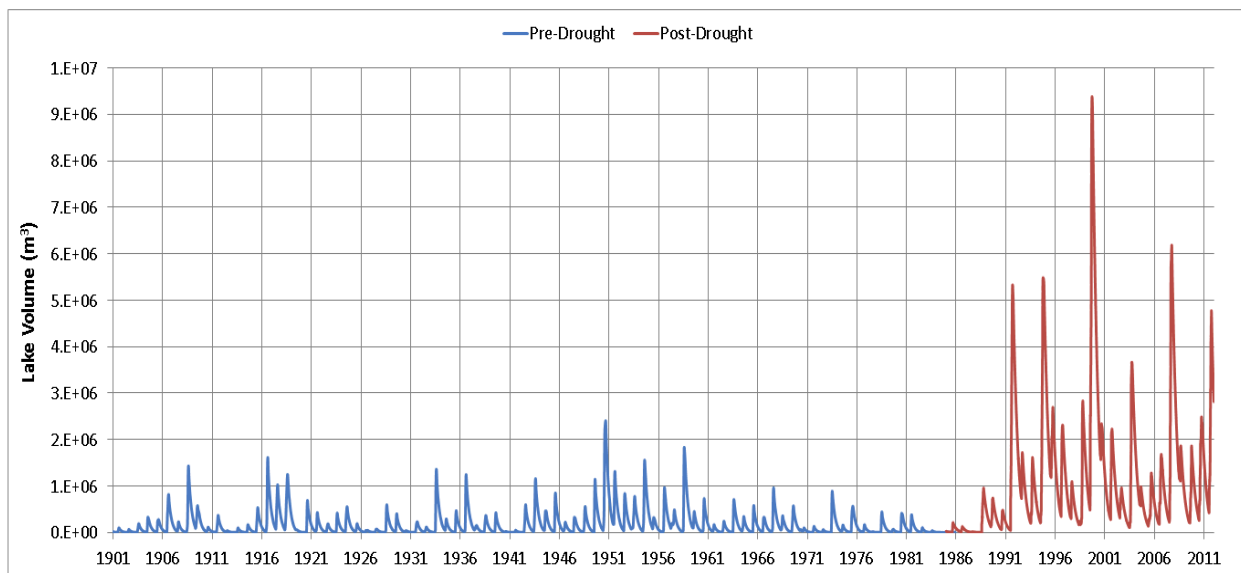


*Figure 4.17*: Simulated lake volume time series for 1901-2011

The purpose of this section is to show that with only mild parameters changes from those used for 1985, the model predicts that Agoufou lake remains ephemeral, further validating the parameters used in *Section 4.2* and providing an interesting look at a different time in Agoufou.

*4.4: Discussion of Project Hypotheses*

       This section will address the questions that have been posed throughout the report. While the main purpose of this entire process was to provide a suitable hydrologic model for socio-eco-hydrologic model coupling purposes in a data-scarce region, we can still try and address some of the main project hypotheses. There are some interesting dynamics at play in the region: eco-hydrologic, climatic, and socioeconomic perturbations have triggered unique paradoxical behavior in a centuries-old prized grazing territory. We seek to understand the connections between these processes, and which, if not all, are the dominant forces driving change.

       Firstly, what are the dominant processes that have caused a lake-state change in Agoufou? As outlined in great detail in the background section of this paper, eco-hydrologic processes set in motion by the Great Sahelian Drought in the mid-1980s devastated woody vegetation populations in the area. 'Tiger bush' (*Figure 4.18*) was prevalent in the North, symbiotically bunching together to create patterns in the shallow sands perpendicular to the drainage direction. Their roots held the sand lenses in place, capturing water for growth and inhibiting surface runoff and erosion. This natural ecosystem had been the norm for many years prior to the GSD.
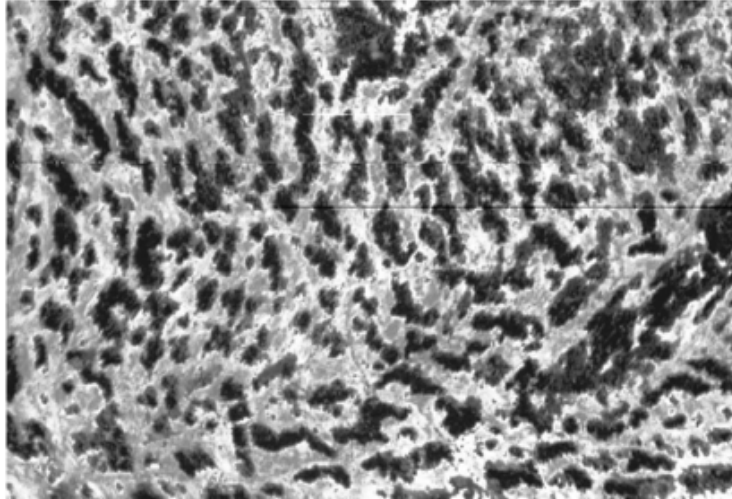
*Figure 4.18*: Tiger bush patterns in the Sahel (*adapted from HAPEX-Sahel*)

Unfortunately for the tiger bush and other woody plant populations in the area, three years of abnormally below average precipitation from 1983-1985 could not sustain their populations. The continental terminal, i.e. hardpan, beneath the sandy soils in which the tiger bush thrived meant that there was no aquifer to replenish the necessary moisture for them to survive. Without woody vegetation roots holding the sandy soils in place, splash erosion from high intensity rainfall brought forth by convective storm systems and blustery winds across the plains exposed more and more of the underlying impervious hardpan. They were not able to recover. With more and more hardpan becoming exposed, the amount of surface runoff increased such that enough water made it into Agoufou lake, causing it to last longer and longer into the dry season until it eventually became perennial.

This eco-hydrologic process is well documented. The ephemeral to perennial lake-state change was almost certainly caused by this chain of events. The more interesting question is this: could the tiger bush have responded to a return in average rainfall by returning had no human intervention occurred? Could the seasonal grazing of the area by

transhumant populations have prevented the tiger bush from returning, or was the tiger bush destined to perish by purely eco-hydrologic factors? And finally, if the tiger bush had returned, would the lake have returned to its previously ephemeral state? These are difficult and interesting questions, and ones we hope to get answers to with a fully coupled model (*see Section 2.2*) addressing all of these influences directly.

However, with what we know now, we can at least hint at an answer to some of these questions. First, we know that there was a 5-6 year period of time between the end of the GSD and when Agoufou first turned perennial. During this 5-6 year period the rains were still below average, with average rains not returning until about 1990 [*Figure 1.4*]. This level of precipitation was enough for annual grasses to blossom, so transhumant populations more than likely continued their seasonal grazing. From *Figure 4.8*, we know that the lake did not start to extend further into the dry season until 1988-1990, so there was no reason for the transhumants to begin to settle yet. Also, the Sahel is a prized grazing resource for its grasses, not for its woody vegetation. The cattle herds would more than likely stick to healthy, moist (*Figure 4.13*) pastures than to venture into an area of sand lenses, hardpan, and dead tiger bush. It is likely that during the 5-6 year period prior to human settlement in the area that if the tiger bush had the ability to recover then it would have. In addition, the fact that tiger bush has seemingly disappeared from the entire region—not just near Agoufou and other sparsely populated area—suggests that tiger bush were wiped out predominantly from eco-hydrologic effects following the GSD. Any interference from human and cattle seems to be secondary to the detrimental effects of the drought. Without tiger bush or some other vegetation reclaiming the northern portion of the basin and decreasing erosion and surface runoff, it seems unlikely that a return to

ephemerality is possible, regardless of increased human settlement and utilization of the basin.

So if human activities did not cause the lake-state transformation nor did they prevent it from reverting to its original state, then are humans increasing the level of degradation and subsequently lake volume or is their effect on the basin minimal? Five to ten thousand cattle and their herders currently reside in and around Agoufou basin. Millet farms fill the area in the flood plain and near other riparian areas where water is readily available. Artificial berms are produced along the stream network to create pools for cattle and farming. Anywhere water flows in significant quantities—i.e. natural or artificial riparian zones—settlements have emerged. The newly released imagery on Google Earth allows a look into the settlements, farming practices, and grazing patterns of cattle in the area [*Figure 4.19*]. It also shows the complex system of surface runoff rills leading from the North into the stream network. There are a few scattered cattle pens but other than that, very few human settlements exist in the barren Northern portion of the basin.

*Figure 4.19*: Aerial imagery of settlements and farming practices near Agoufou Lake (*Google Earth*)

There is no doubt that near the riparian areas and in cattle pens the infiltrability of the soils has been decreased by repeated use. Poor farming practices could also lead to erosion of the topsoil layer. The runoff ratios of those areas have increased—that is a fact. However, the relative area of human settlement to basin area is quite small. In *Section 4.1 Figure 4.3,* 82% of runoff into Agoufou Lake consisted of surface flow. Well over 90% of all surface runoff originates from the Northern portion of the basin. *Figures 4.4 & 4.5* tell the story visually. Following a 75 mm rainstorm, the surface runoff response of the North portion of the basin trumps the subsurface response of the South. The large dunes of the South provide a huge storage volume (*Figure 4.6, 4.13, 4.16*) that acts as a sponge for rainwater. Barring increased urbanization of the Southern portion of the basin: expanded

farming, increased number of buildings and roads, and overall population explosion, the relative degradation of the basin caused by humans does not seem to be greater than the eco-hydrologic effects of the past 30 years.

## 5. Summary and Conclusions

Over the past 30 years since the Great Sahelian Drought (GSD) of 1983-1985, a hydrologic regime shift has occurred in the small lake basin of Agoufou. In the early 1990s, the ephemeral pond that had existed in Agoufou for the years prior to the GSD became a perennial lake. This system-level change set into motion a reorganization of the human interaction in the region—once only seasonal grazing occurred, but with the presence of a perennial lake, permanent settlements began to arise. In the years since the lake-state change, the lake volume has continued to increase despite no increase in average rainfall over the same period. Interesting questions have arisen as to why the lake-state change occurred in the first place, and to why the volume in Agoufou Lake continues to rise.

While the original lake-state change is widely attributed to eco-hydrologic effects of the GSD involving woody vegetation die-off and subsequent erosion of surface soils leading to increased surface runoff, the effect of human settlement on basin hydrologic response in Agoufou has yet to be studied intensively. Logically, it was hypothesized that increased human interaction in the basin may have ensured that the lake could not revert to its original equilibrium state. In addition, it was postulated that increased agro-pastoral activities in the basin might be contributing to the increased lake volumes. Finally, are humans the dominant players of eco-hydrologic change in the area, do they play a secondary role, or are their impacts negligible?

Human settlement did not occur immediately following the lake-state change of Agoufou after the GSD, it has slowly grown over the last 20 years. At first, settlements began to appear directly adjacent to the lake. Only once that area had been filled did further expansion to the riparian areas feeding Agoufou Lake begin to fill with settlements. Yet, the

largest increase in lake volumes relative to previous years occurred in the early to mid 1990s, before human settlement had reached present-day levels. Since surface runoff from the North became the dominant form of runoff soon after the GSD, this seems to indicate that increases in degradation of vegetation and soil of the North were occurring prior to humans settling in the area. Given this information, it was concluded that human settlement did not have a major effect on the ability of the basin to revert to its previously ephemeral state—purely eco-hydrologic effects were the cause of the apparently irreversible system change.

Human agro-pastoral interaction with the basin is limited mainly to the riparian zones and in the South where grasses dominate in the wet season. However, the model simulations predict that the majority of the volume of hydrologic response post-GSD is due to surface runoff from hardpan sections in the North. The Northern portion of the basin does not provide much grassy vegetation for cattle to graze, nor does it contain soils suitable for agriculture. Therefore, human interaction with the North is minimal. The area of basin that is affected by human settlement is primarily limited to riparian areas in the South for farming, and Southern savannah grasses for grazing. Even prior to the lake-state change, cattle grazed the grasses yearly. No noticeable change to the viability of savannahs of the South has occurred due to year-round grazing by cattle. Each year, the grasses return in full force in response to the return of the rains. The hydrologic response in the form of runoff due to the increased grazing is negligible compared to runoff from the north. The majority of the precipitation that falls in the South still infiltrates into deep sand dunes and is then evaporated. Surface runoff from riparian zones that have been degraded by human settlement has increased, but the area is negligible to the impervious hardpan areas of the

North that increase in size each year due to wind and splash erosion. The results from simulations of Agoufou seem to reveal that at the current level of human interaction in the area, their impact on basin change is secondary to the irreversibly detrimental effects of woody vegetation die-off in the North following the GSD.

# 6. References

Bouchet, R. J., Evapotranspiration r´eelle evapotranspiration potenti-elle, signification climatique, Int. Assoc. Sci. Hydrol., Berkeley, Ca- lif., Symp. Publ. 62, pp. 134–142, 1963.

Brutsaert, W., and H. Stricker, An advection-aridity approach to esti- mate actual regional evapotranspiration, Water Resour. Res., 15(2), 443–450, 1979.
Dembele, F., Picard, N., Karembe, M. and Birnbaum, P., 2006. Tree vegetation patterns along a gradient of human disturbance in the Sahelian area of Mali. Journal of Arid Environments, 64(2): 284-297.

Descroix L., Mahé G., Lebel T., Favreau G, Galle S., Gautier E., Olivry J.C, Albergel J, Amogu O., Cappelaere B., Dessouassi R., Diedhiou A., Le Breton E., Mamadou I., Sighomnou D., 2009. Spatio-temporal variability of hydrological regimes around the boundaries between Sahelian and Sudanian areas of West Africa: a synthesis. J. Hydrol, 375, (1-2), 90-102.

Favreau G., B. Cappelaere, S. Massuel, M. Leblanc, M. Boucher, N. Boulain, C. Leduc., 2009. Land clearing, climate variability, and water resources increase in semiarid south-west Niger, Africa: a review. Water Resources Research , 45, W00A16, doi:10.1029/2007WR006785.

Favreau, G., Leduc, C., Marlin, C., Dray, M., Taupin, J.D., Massault, M., Le Gal La Salle, C. and Babic, M., 2002. Estimate of recharge of a rising water-table in semi-arid Niger from 3H and 14C modelling. Ground Water, 40(2): 144-151.

Frappart, F., Hiernaux, P., Guichard, F., Mougin, E., Kergoat, L., Arjounin, M., Lavenu, F., Koité, M., Paturel, J.-E., Lebel, T.. Rainfall regime over the Sahelian climate gradient in the Gourma, Mali. J. Hydrology, 375, 1-2, 128-142.

Gardelle, J., Hiernaux, P., Kergoat, L. and Grippa, M., 2009. Less rain, more water in ponds: a remote sensing study of the dynamics of surface waters from 1950 to present in pastoral Sahel (Gourma region, Mali). Hydrology and Earth System Sciences Discussions, 6: 5047-5083.

Gardelle, J., Hiernaux, P., Kergoat, L. and Grippa, M., 2009. Less rain, more water in ponds: a remote sensing study of the dynamics of surface waters from 1950 to present in pastoral Sahel (Gourma region, Mali). Hydrology and Earth System Sciences Discussions, 6: 5047-5083.

GW Geeves, B Craze, GJ Hamilton – 2007a - Oxford University Press. Soil physical properties. In 'Soils: their properties and management,.(Eds PEV Charman, BW Murphy) pp. 168-191
Hapex-Sahel (Lara/Pierre/etc.)
Hargreaves, G.H. and Z.A. Samani. 1982. Estimating potential evapotranspir- ation. Tech. Note, J. Irrig. and Drain. Engr. 108(3):225-230.

Hiernaux, P., Diarra, L., Trichon, V., Mougin, E., Soumaguel, N., Baup, F., Woody plant

population dynamics in response to climate changes from 1984 to 2006 in Sahel (Gourma, Mali), Journal of Hydrology (2009), doi: 10.1016/j.jhydrol.2009.01.043

Hiernaux, P., Gerard, B., 1999. The influence of vegetation pattern on the productivity, diversity and stability of vegetation: The case of 'brousse tigrée' in the Sahel. Acta Oecologica, 20(3), 147-158.

Hobbins et al. The complementary relationship in estimation of regional evapotranspiration: The Complementary Relationship Areal Evapotranspiration and Advection-Aridity models. Water Resources Research, 37, 5, 1367–1387, 2001.

Hoogmoed, W.B. and Stroosnijder, L. 1984. Crust formation on sandy soils in the Sahel. I. Rainfall and infiltration. Soil Tillage Res. 4:5-23

Kaptue Tchuente, Armel Thibaut, Jean-Louis Roujean, and Stéphanie Faroux. "ECOCLIMAP-II: An ecosystem classification and land surface parameters database of Western Africa at 1km resolution for the African Monsoon Multidisciplinary Analysis (AMMA) project." Remote Sensing of Environment114.5 (2010): 961-976.
Le Barbé, L., Lebel, T. and Tapsoba, D., 2002. Rainfall variability in West Africa during the years 1950-90. J. Climate, 15: 187-202.

Book: Le Houérou, H.N., 1989. The Grazing Land Ecosystems of the African Sahel. Ecological Studies, 75. Springer-Verlag, Berlin.

Le Houérou, H.N., 1980. The rangelands of the Sahel. Journal of Range Management, 33(1): 41- 46.

Lebel, T., J.-D. Taupin, and N. D'Amato (1997), Rainfall monitoring during Hapex-Sahel. 1. General rainfall conditions and climatology, J. Hydrol., 188–189, 74–96, doi:10.1016/S0022-1694(96)03155-1.

Leblanc, M., Favreau, G., Massuel, S., Tweed, S., Loireau, M. and Cappelaere, B., 2008. Land clearance and hydrological change in the sahel: SW Niger. Global and Planetary Change, 61: 135-150.

Leduc, C., Favreau, G. and Schroeter, P., 2001. Long term rise in a Sahelian water-table: the Continental Terminal in South-West Niger. Journal of Hydrology, 243: 43-54.

Mahé G, Leduc C., Amani A., Paturel J.E., Girard S., Servat E., Dezetter A., 2003. Augmentation du ruissellement de surface en région soudano-sahélienne et impact sur les resources en eau. In Hydrology of Mediterranean and Semiarid regions, Servat E., Najem W., Leduc C., Shakeel A. (Sci. Eds), Proc. Conf., Montpellier, France, 003, IAHS Pub., 278, 215-222.

Mahé G., Olivry J.C., Servat E., 2005 (a). Sensibilité des cours d'eau ouest africains aux changements climatiques et environnementaux : extrêmes et paradoxes. In Regional hydrological impacts of climatic change - hydroclimatic variability. proceedings of

symposium S6 held during the seventh IAHS scientific Assembly at Foz de Iguaçu, Brazil, April 2005, IAHS pub., 296, 169- 177.

Mathon, V., Laurent, H. and Lebel, T., 2002. Mesoscale convective system rainfall in the Sahel. J. Applied Meteo., 41: 1081-1092.

Mitchell, T.D., 2004: An improved method of constructing a database of monthly climate observations and associated high resolution grids.
Monteith, J.L. 1965. Evaporation and the environment. p. 205-234. In The state and movement of water in living organisms. 19th Symposia of the Society for Experimental Biology. Cambridge Univ. Press, London, U.K.

Morton, F. I., Operational estimates of areal evapotranspiration and their significance to the science and practice of hydrology, J. Hydrol., 66, 1–76, 1983.

Mougin, E. et al., 2009. The AMMA Gourma observatory site: an overview of research activities. J. Hydro., this issue.

Neitsch et al. 2011. Soil and Water Assessment Tool Version 2009

Nicholson, S., 2005. On the question of the "recovery" of the rains in the West African Sahel. Journal of Arid Environments, 63(3): 615-641.

Nicholson, S.E., 2001. Climate and environmental change in Africa during the last two centuries. Clim. Res., 14, 123-144.

Novella, Nicholas, and Wassila Thiaw. "9B. 6: Africa Rainfall Climatology Version 2." NOAA.
Olsson L., 1993. On the causes of famine: drought, desertification and market failure in the Sudan. Ambio 22, 395-403

Olsson, L., Eklundh, L. and Ardo, J., 2005. A recent greening of the Sahel - Trends, patterns and potential causes. Journal of Arid Environments, 63(3): 556-566.

Penman, H. L., Natural evaporation from open water, bare soil and grass, Proc. R. Soc. London, Ser. A., 120–146, 1948.

Priestley, C.H.B. and R.J. Taylor. 1972. On the assessment of surface heat flux and evaporation using large-scale parameters. Mon. Weather Rev. 100:81-92.

Sharpley, A.N. and J.R. Williams, eds. 1990. EPIC-Erosion Productivity Impact Calculator, 1. model documentation. U.S. Department of Agriculture, Agricultural Research Service, Tech. Bull. 1768.

Turner, M.D., 2000. Misunderstandings of Sahelian land use ecology. In: T. Singh (Editor), Environment: Reality and myth. A symposium re-evaluating some prevailing beliefs.

Valentin, C., Rajot, J.L., Mitja, D., 2004. Responses of soil crusting, runoff and erosion to

fallowing in the subhumid and semi-arid regions of West Africa. Agriculture, Ecosystems and Environment 104, 287-302.

Williams, J.R. 1995. Chapter 25: The EPIC model. p. 909-1000. In V.P. Singh (ed.). Computer models of watershed hydrology. Water Resources Publications.